The Development of Magmatism Along the Cameroon Volcanic Line: Evidence from Teleseismic Receiver Functions

R. J. Gallacher,[1] I. D. Bastow,[1]

R. J. Gallacher, School of Earth Sciences, University of Bristol, Bristol, BS8 1RJ, UK

I. D. Bastow, School of Earth Sciences, University of Bristol, Bristol, BS8 1RJ, UK. (ian.bastow@bristol.ac.uk)

[1]School of Earth Sciences, University of Bristol, Bristol, BS8 1RJ, UK

Abstract. The Cameroon Volcanic Line (CVL) in West Africa is a chain of Cenozoic volcanism with no clear age progression. The reasons for its existence are unclear and the nature of its magmatic plumbing system is poorly understood. Specifically, whether or not the CVL crust presently contains melt and/or mafic intrusions, as is often observed at hotspots and rifts elsewhere, is presently unknown. To address this issue, we present a receiver function study of crustal structure using earthquakes recorded by the Cameroon Broadband Seismic Experiment. In regions of the CVL unaffected by Cretaceous extension associated with the breakup of Gondwana (e.g., the Garoua rift), Vp/Vs ratios are markedly low (network average ∼1.74) compared to hotspots elsewhere, providing no evidence for either melt, or cooled mafic crustal intrusions due to CVL magmatism. The character of P-to-S conversions from beneath the CVL also indicates that lower-crustal intrusions (often termed underplate) are not present beneath the region. Our observations thus corroborate earlier petrological studies that show CVL alkaline magmas fractionate in the mantle, not the crust, prior to eruption. Hypotheses for the formation of the CVL should not include markedly elevated upper-mantle potential temperatures, or large volumes of partial melt, both of which can explain observations at hotspots and rifts worldwide. The protracted, yet sporadic development of small-volume alkali melts beneath the CVL may instead be explained better by lower melt volume mechanisms such as shear zone reactivation or lithospheric delamination.

1. Introduction

1.1. Overview

The Cameroon Volcanic Line (CVL) is a region of intra-plate volcanism, with no evidence for age progression, that straddles the continent-ocean boundary in central West Africa [Figure 1: e.g., *Fitton*, 1980; *Halliday et al.*, 1990; *Nkouathio et al.*, 2008]. The reasons for the existence of the chain have long been debated, with end-member hypotheses including traditional mantle plumes [e.g., *Lee et al.*, 1994; *Burke*, 2001; *Ngako et al.*, 2006], decompression melting beneath reactivated shear zones in the lithosphere [e.g., *Freeth*, 1979; *Fairhead*, 1988; *Fairhead and Binks*, 1991; *Moreau et al.*, 1987], and small-scale upper-mantle convection [e.g., *King and Anderson*, 1995, 1998; *King and Ritsema*, 2000] each having been proposed for the region. It has also been suggested that lateral flow of buoyant asthenosphere, beneath continental lithosphere thinned extensively during Mesozoic rifting, may now be contributing to the younger volcanism along the line [*Ebinger and Sleep*, 1998]. Analogies with other hotspot chains worldwide are thus not well established and the nature of the CVL's magmatic plumbing system remains relatively poorly understood.

One aspect of CVL magmatism that is now well established is the composition of its Oligocene-to-Recent lavas. Petrological studies show that the CVL's mostly basaltic volcanoes have erupted alkaline basalts in relatively low volume [e.g., *Fitton*, 1980; *Suh et al.*, 2003]. These silica poor lavas have not undergone appreciable fractionation at depth, which raises the question of whether or not the crust beneath the CVL is characterized by cooled mafic intrusions and/or present-day melt, as is often observed at hotspots and rifts worldwide [e.g., *Ebinger and Casey*, 2001; *Maguire et al.*, 2006; *Thybo and Nielsen*, 2009]. To help address this question, and to place fundamental new constraints on melt supply beneath the CVL, we perform a receiver function study of bulk crustal seismic structure (Moho depth, H and Vp/Vs ratio, κ) using distant earthquakes recorded by the Cameroon Broadband Seismic Experiment [CBSE: e.g., *Reusch et al.*, 2010] between 2005 and 2007. The network samples crust that spans more than 3 billion years of the geological record in Cameroon, from Congo Craton basement formation during the Archean, to volcanism along the CVL during Holocene times.

If the crust beneath the CVL is host to appreciable volumes of melt and mafic crustal intrusion, this should be manifest as elevated bulk crustal Vp/Vs ratios, as is observed at hotspots and magmatic rifts such as Iceland [e.g., *Darbyshire et al.*, 1998] and Ethiopia [e.g., *Stuart et al.*, 2006], respectively. Lower crustal intrusions (with or without present-day melt) can also be identified using the receiver function technique via analysis of the amplitude and shape of P-to-S conversions from the Moho [e.g., *Stuart et al.*, 2006; *Zheng et al.*, 2008]. Our fundamental new constraints on Cameroon's bulk crustal seismic structure thus allow us to draw comparisons with rifts and hotspots worldwide, where the reasons for magmatism are relatively well established. Better constraints on the CVL magmatic plumbing system lead, in turn, to a better understanding of the mechanism of melt development in the mantle beneath the line.

1.2. Geological and Tectonic Setting

The oldest rocks in Cameroon are found within the 2.5–3.0 b.y. old Archean Congo craton in the SW of the country [Figure 1; e.g., *Cahen et al.*, 1984; *Nzenti et al.*, 1988;

Tchameni et al., 2001]. The northernmost exposure of the craton in Cameroon is known as the Ntem Complex (Figure 1), which consists of Archean-age greenstone terranes, surrounded by tonalitic, trondhjemitic and granodioritic rocks [e.g., *Tchameni et al.*, 2000]. Parts of the region were re-worked in Paleoproterozoic times with mafic doleritic intrusions modifying the crust [e.g., *Tchameni et al.*, 2001].

The Proterozoic Oubanguides Belt, comprising metamorphosed schists and gneisses, lies to the north of the Congo Craton. It forms part of the larger Neoproterozoic Pan African–Brazilian Belt, which underwent significant deformation during the Pan African Orogeny ca. 600 Ma when the Congo, São Francisco and West African Cratons collided during the formation of Gondwana [e.g., *Toteu et al.*, 1987; *Nzenti et al.*, 1988; *Toteu et al.*, 2001; *Oliveira et al.*, 2006]. During the collision, Proterozoic sediments were thrust on top of the edge of the Congo Craton ca. 565 Ma [e.g., *Toteu et al.*, 1987; *Nzenti et al.*, 1988; *Ngako et al.*, 2006] such that its northern edge is now buried beneath the Yaoundé domain [Figure 1; e.g., *Toteu et al.*, 1987; *Oliveira et al.*, 2006].

Cross-cutting the Proterozoic Oubanguides Belt are several major shear zones, including the Central African Shear Zone (CASZ), a major tectonic feature that can be traced across the African continent from Sudan towards the Adamawa Plateau [e.g., *Guiraud et al.*, 1992; *Binks and Fairhead*, 1992] and into SW Cameroon, where it is masked by Cenozoic volcanic rocks (Figure 1).

The breakup of Gondwana ca. 125 Ma resulted in the separation of Africa and South America, and the formation of the South Atlantic [e.g., *Burke and Dewey*, 1973]. At this time, SW Cameroon and the region that is now the Gulf of Guinea was characterized by a triple junction, the third arm of which formed the Benue Trough, a continental rift that subsequently failed to develop [e.g., *Burke et al.*, 1971]. The Garoua rift (Figure 1) marks the eastward extension of the Benue Trough into northern Cameroon. The opening of the South Atlantic also resulted in reactivation of the CASZ [e.g., *Binks and Fairhead*, 1992; *Browne and Fairhead*, 1983], which is known on the conjugate rifted margin in Brazil as the Pernambuco lineament [e.g., *Oliveira et al.*, 2006]. The CASZ consists of many individual shear zones that formed extensional basins during Cretaceous times to accommodate stress transferred to the African continental interior during the opening of the South Atlantic [e.g., *Browne and Fairhead*, 1983].

Since Oligocene times, Cameroon has experienced sporadic volcanism along the CVL, which trends SW–NE and extends ∼1600 km from offshore in the Gulf of Guinea to Lake Chad [Figure 1: *Fitton*, 1980; *Halliday et al.*, 1988; *Déruelle et al.*, 2007; *Nkouathio et al.*, 2008], with an additional E-W trending arm at ∼7°N that extends across the Adamawa Plateau (Figure 1). The CVL is underlain by Pan African basement rocks consisting of schists and gneisses intruded by granites and diorites [e.g., *Fitton*, 1987; *Déruelle et al.*, 2007]. Magmatism along the CVL began ca. 30 Ma at the Mandara Mountains and on the Island of Principe [e.g., *Halliday et al.*, 1988] but there is no evidence for age progression along the line [e.g., *Fitton and Dunlop*, 1985; *Halliday et al.*, 1988]. Table 1 shows a summary of the timing of CVL volcanism, compiled by *Halliday et al.* [1988].

Fitton and Dunlop [1985] showed using the elemental compositions of basaltic lava collected along the CVL, that magmas along the continental and oceanic sectors of the line are very similar. This led them to the conclusion that there is a single mantle source along the chain, a hypothesis supported by several subsequent studies [e.g., *Halliday et al.*, 1988; *Rankenburg et al.*, 2005; *Déruelle et al.*, 2007]. Petrological data also show that hawaiite and basanite alkali basaltic volcanism is commonplace along the CVL. These low-volume, high-pressure lavas suggest that little shallow (crustal) fractionation of magma is occurring beneath the line prior to eruption [e.g., *Fitton and Dunlop*, 1985; *Halliday et al.*, 1988; *Marzoli et al.*, 2000; *Suh et al.*, 2003; *Yokoyama et al.*, 2007; *Déruelle et al.*, 2007; *Njonfang et al.*, 2011; *Teitchou et al.*, 2011].

1.3. Previous Geophysical Work

The lithospheric seismic structure of Cameroon has been determined by continent-scale surface-wave studies [e.g., *Pasyanos and Nyblade*, 2007; *Priestley et al.*, 2008; *Fishwick*, 2010]. They indicate that the CVL is underlain by mantle characterized by slow seismic wave-speeds and that the lithosphere-asthenosphere boundary beneath the Congo Craton is at a depth of $\sim$250 km. In contrast, the lithosphere is $<$100 km thick beneath the CVL [*Fishwick*, 2010].

Pérez-Gussinyé et al. [2009] constrain effective elastic plate thickness (a proxy for lithospheric strength) across Africa using coherence analysis of topography and Bouguer anomaly data. The weakest lithosphere is found in Ethiopia and is attributed both to the low wave-speed, hot mantle beneath the region, and the large degree of extension in that part of the East African rift system. Channels of relatively weak lithosphere extend across the African continent from this region to the CVL, where the effective elastic plate thickness is also relatively low compared to the surrounding areas. This was cited by *Pérez-Gussinyé et al.* [2009] as evidence in support of the model of *Ebinger and Sleep*

[1998], who proposed that flow of buoyant asthenosphere beneath continental lithosphere thinned extensively during Mesozoic rifting may now be contributing to volcanism along the CVL.

On a more local scale in Cameroon, *Dorbath et al.* [1986] analysed teleseismic P-wave travel-time residuals recorded by a 300 km-long profile of 40 short period seismograph stations across the Adamawa Plateau. Using these data they identified upper-mantle wave-speed contrasts of $<$2.5% across the Plateau (Figure 1), an observation they cite as evidence for the presence of a mantle thermal anomaly. *Plomerova et al.* [1993] analysed data from the same seismic array and found evidence for $\sim$70 km lithospheric thinning beneath the Adamawa Plateau in the region where it is cross-cut by the CASZ. In support of these teleseismic studies, gravity **studies** by *Poudjom Djomani et al.* [1997] and *Nnange et al.* [2001] also found evidence for localized low density mantle beneath the region.

Most recently, *Reusch et al.* [2010] used body wave tomography to image the mantle seismic structure beneath Cameroon using data from the 2005–2007 CBSE experiment. They found that a continuous low velocity zone ($\delta V_S = -2$ to -3%) underlies the entire CVL to a depth of at least 300 km and attributed this to a thermal anomaly of at least 280 K.

Within Cameroon, gravity maps have often been used to delineate tectonic subdivisions inaccessible by traditional field geology due to younger sediment cover [e.g., *Fairhead and Okereke*, 1987; *Poudjom Djomani et al.*, 1992; *Djomani et al.*, 1995; *Poudjom Djomani et al.*, 1997; *Toteu et al.*, 2004; *Tadjou et al.*, 2009; *Shandini et al.*, 2010; *Basseka et al.*, 2011]. A steep gradient in the Bouguer gravity field at $\sim$4°N and $\sim$10°E within the

Yaoundé domain (Figure 1), for example, has been interpreted by these **researchers** as the sediment-covered edge of the Congo Craton.

The earliest seismological constraints on crustal thickness in Cameroon came from *Stuart et al.* [1985], who used direct as well as reflected and refracted waves from quarry blasts to determine a crustal thickness of $\sim$33 km beneath the Adamawa Plateau, which has an upper-mantle P-wave velocity of $\sim$8 kms^{-1}. They also show that the crustal thickness in the Garoua Rift is $\sim$23 km with an upper-mantle P-wave velocity of $\sim$7.8 kms^{-1}. More recently, *Tokam et al.* [2010] conducted a joint receiver function and surface-wave study of crustal structure across Cameroon using data from the CBSE network. Average shear wave velocity across Cameroon was found to be $\sim$3.7 kms^{-1} and mean crustal thickness $\sim$36 km. Beneath the Garoua Rift and towards the coast, the crust was found to be significantly thinner at 26-31 km. In contrast, the Congo Craton in Cameroon has thicker crust (43–48 km) and elevated mean crustal seismic velocities (3.9 kms^{-1}). The CVL and Oubanguides belt are characterized by crustal thicknesses of 35-39 km. Thickened crust and a $\sim$25 km-thick high-velocity lower-crustal layer beneath the northern margin of the Congo Craton was attributed to the collisional tectonic processes that characterized the formation of Gondwana. *Tokam et al.* [2010] also suggested that thin bodies of mafic material exist in the top 10–15 km of the crust throughout Cameroon.

Cameroon is relatively aseismic compared to magmatically active regions such as Ethiopia [*Keir et al.*, 2009; *Ebinger et al.*, 2010] in East Africa. However, studies of seismicity around Mount Cameroon, site of the most recent eruption along the CVL [e.g., *Ateba et al.*, 2009], show that earthquakes occur at depths as great as 55–60 km in the sub-continental lithospheric mantle [*Tabod et al.*, 1992; *Ateba and Ntepe*, 1997]. For a review of recent seismological work in Cameroon, see *Fishwick and Bastow* [2011].

2. Method

Data were obtained from 32 broadband stations throughout the CBSE network, spanning the continental sector of the Cameroon Volcanic Line and the boundary with the Congo Craton (Figure 1). The CBSE was run between January 2005 and February 2007 and the stations were positioned ∼50–150 km from each other [*Reusch et al.*, 2010]. A second order Butterworth filter with corner frequencies of 0.04 and 3 Hz was applied to the data prior to analysis. Quality control was subsequently performed on the data such that only traces with a high signal-to-noise ratio and P arrivals were used. This resulted in a data set of 158 earthquakes which range between 3 and 18 per station (Figure 2).

Receiver functions capture P-to-S wave conversions at velocity contrasts in the receiver crust and mantle that are recorded in the P-wave coda from teleseismic earthquakes [*Langston*, 1977]. The receiver function method used in this study is the Extended-Time Multitaper Frequency-Domain Cross-Correlation Receiver-Function (ETMTRF) approach of *Helffrich* [2006]. This uses short multiple tapers which window the full length of the time series. This adds all of the Fourier transforms in the frequency domain such that the phase lags of each sub-window are preserved. The travel times of P-to-S conversions at the Moho can be studied to provide information on the crustal thickness (H) and Vp/Vs ratio (κ). This is achieved with the stacking procedure outlined by *Zhu and Kanamori* [2000]. Both a linear [*Zhu and Kanamori*, 2000] and a phase weighted stacking [PWS: *Schimmel and Paulssen*, 1997] approach were used to verify the results. The linear approach uses Equation 1 for stacking, in conjunction with the equations for the predicted travel times (Equations 2-4). This results in a grid which gives the plausible range of values for H and κ between, 20–60 km and 1.6–2.2 respectively:

$$s(H,\kappa) = \sum_{j=1}^{N} w_1 r_j(t_1) + w_2 r_j(t_2) - w_3 r_j(t_3), \tag{1}$$

where ω_1, ω_2 and ω_3 are weights, $r_j(t_i)$ are the amplitudes at the arrival times for each of the ray paths evaluated. N is the number of receiver functions:

$$t_1 = H\left[\sqrt{\frac{1}{V_S^2} - p^2} - \sqrt{\frac{1}{V_P^2} - p^2}\right], \tag{2}$$

$$t_2 = H\left[\sqrt{\frac{1}{V_S^2} - p^2} + \sqrt{\frac{1}{V_P^2} - p^2}\right], \tag{3}$$

$$t_3 = 2H\sqrt{\frac{1}{V_S^2} - p^2}, \tag{4}$$

where p is the ray parameter. For phase weighted stacking, the linear approach is altered by adding the factor c, which is a measure of the correlation of the data between 0 and 1:

$$c(H,\kappa) = \frac{1}{N}\sum_{j=1}^{N} \frac{\left|\sum_{\kappa=1}^{3} e^{i\Phi(t_\kappa)}\right|}{3}, \tag{5}$$

where Φ is the instantaneous phase at time t. This is then combined with Equation 1 to give:

$$s(H,\kappa) = c^v \sum_{j=1}^{N} w_1 r_j(t_1) + w_2 r_j(t_2) - w_3 r_j(t_3), \tag{6}$$

where the value of v controls the sharpness of the filtering by c, between poorly correlated and well correlated data. The value for v was taken to be 2 throughout the analysis as this provided sharper output than a value of 1, consistent with the studies of *Schimmel and Paulssen* [1997] and *Thompson et al.* [2010]. The weights were chosen as ω_1=0.5, ω_2=0.4 and ω_3=0.1, as the P-to-S and PpPs transitions are much clearer than the PpSs+PsPs transition. The errors in the results were calculated by taking the maximum axes of the 95% confidence interval of the grid plotted using the *Zhu and Kanamori* [2000] stacking method, where the H-κ grid consists of 10000 points (Figure 3).

3. Results

Of the 32 CBSE stations, 24 yielded receiver functions with a coherent P-to-S arrival. Of these, **18** displayed PpPs and PpSs+PsPs arrivals, thus enabling H-κ analysis. The phase weighted stacking and linear methods yielded similar results with differences of no more than 0.8 km for H and 0.06 for Vp/Vs (Table 2). Errors in the linear method were slightly higher than those for the phase weighted stacking method, with differences of <0.7 km for δH and 0.03 for δVp/Vs. Examples of stacked receiver functions and H-κ plots for stations CM22 and CM29 are shown in Figure 3. For the **6** stations at which no clear reverberant phases were found, receiver functions were combined to form single station stacks. Crustal thicknesses were then determined using Equation 2 assuming Vp/Vs ratio from the nearest station constrained by H-κ analysis.

Six stations in the south of Cameroon (CM02–CM04, CM06, CM07, CM11) have a crustal thickness of >40 km (Figure 4). Other nearby stations (CM01, CM05, CM10, CM12, CM17) have markedly thinner crust **(H ≈ 37** km: Figure 4). Most of the southern stations (e.g., CM02, CM03, CM07, CM10, CM12, CM17) have extremely low Vp/Vs ratios of 1.65-1.73 (Figure 5). Exceptions to this are stations CM04 and CM06 in the Ntem Complex (Vp/Vs = 1.78 and 1.82, respectively). Transects A–A' and B–B' (Figure 6) show the abrupt change in crustal thickness of ∼5 km and the lack of variation in Vp/Vs ratios between the CVL and neighbouring Congo Craton. Throughout the CVL and central Cameroon (CM13, CM16, CM20–CM27), crustal thickness is ∼34–39 km (Figure 4); Vp/Vs ratios are generally low at 1.67-1.76 (Figure 5). Transect C-C' show the consistently low Vp/Vs ratios along the CVL (Figure 6).

While most of the study area is characterized by relatively low Vp/Vs ratios (network mean Vp/Vs = 1.74) compared to the global mean of 1.768 [*Christensen*, 1996], localized exceptions, in addition to CM04 and CM06, include CM29, CM30 and CM32 near the Garoua Rift (Figure 1) in the northern part of the study area; these have Vp/Vs ratios of 1.75-1.84; the crust is also thinner in this region (H = 25–33 km: Figure 4 & 6).

4. Discussion

4.1. Comparison with Previous Studies and Implications for Tectonic Subdivisions

Many of the tectonic subdivisions in Cameroon are based entirely on analysis of potential field data such as gravity studies [e.g., *Fairhead and Okereke*, 1987; *Djomani et al.*, 1995]; mapping by traditional field geology is often not possible because the putative terrane boundaries are covered by younger rocks [e.g., *Basseka et al.*, 2011]. For example, the northern edge of the Congo Craton lies beneath thick Proterozoic sediments in the Yaoundé domain (Figure 1) that were thrust on top of it ca. 565 Ma during the formation of Gondwana [e.g., *Toteu et al.*, 1987; *Nzenti et al.*, 1988; *Ngako et al.*, 2006]. A sharp crustal boundary identified as a steep gradient in the Bouguer gravity field at $\sim$4°N appears to constrain the northern edge of the Congo craton at depth [e.g., *Fairhead and Okereke*, 1987; *Djomani et al.*, 1995; *Poudjom Djomani et al.*, 1997; *Toteu et al.*, 2004; *Tadjou et al.*, 2009; *Shandini et al.*, 2010; *Basseka et al.*, 2011]. Consistent with these studies, we observe an abrupt change in crustal thickness at the same latitude. The average crustal thickness at stations CM02–CM04, CM06–CM07, and CM11 is $\sim$44 km, but north of $\sim$4°N it is consistently $\leq$38 km (Table 2, Figures 4 and 6). When reviewed in light of other geophysical constraints, including the receiver function study of *Tokam et al.* [2010], our results thus confirm that the northern limit of the Congo Craton is likely $\sim$4°N, and its eastern limit in Cameroon $\sim$10°E.

In cratonic southern Cameroon, Vp/Vs ratios at stations CM04 and CM06 (Figure 5) within the Archean Ntem complex (Figure 1) are elevated (Vp/Vs = 1.78 and 1.82, respectively) compared to the values usually encountered in cratonic regions [e.g., $\sim$1.725 for Paleoarchean Rae domain of northern Canada: *Thompson et al.*, 2010]. The Ntem complex has been unaffected by volcanism associated with the Cretaceous breakup of Gondwana, and the subsequent development of the CVL; thus neither of these tectonic processes can explain the observations. Instead, mafic intrusion during the Neoarchean emplacement of greenstone terranes [e.g., *Tchameni et al.*, 2000] may have elevated Vp/Vs ratios compared to the surrounding relatively felsic cratonic crust at stations such as CM02, CM03 and CM07 where Vp/Vs = 1.65–1.73 (Figure 5). A similar hypothesis was proposed by *Thompson et al.* [2010] to explain observations in the greenstone terranes of the ∼2.7 Ga Hearne domain in Canada, where Vp/Vs ratios are slightly higher at ∼1.76 than in the neighboring Paleoarchean Rae domain (Vp/Vs = 1.725). Additionally, mafic material may have been assimilated into the crust during collisional tectonics during the formation of Gondwana. This latter hypothesis was also proposed by *Tokam et al.* [2010], who cited high-velocity lower-crust in this region as evidence for mafic magmatic addition during the Pan African orogeny.

Previous studies of Precambrian terranes worldwide indicate that average Archean crust is thinner than average Proterozoic crust [∼35 km and ∼45 km respectively; *Durrheim and Mooney*, 1991], with thicker Archean terranes generally the site of ancient collisional boundaries. On the other hand *Tedla et al.* [2011] used surface and satellite gravity data to produce a crustal model for Africa that shows average crustal thickness for the continent is almost identical to that of the Archean and Proterozoic domains within it (each ∼39 km). Since our constraints on crustal thickness of the Congo Craton are on its rifted margins, not its deep interior, we cannot determine with confidence the extent to which collisional processes during the Pan African Orogeny have served to thicken the crust compared to the neighbouring Proterozoic crust.

In the northern part of the study area, the Garoua Rift marks the eastward extension of the Benue Trough into northern Cameroon. Rifting here developed in Cretaceous times during the breakup of Gondwana. Several gravity and seismic field experiments have been conducted both here and across the nearby Adamawa Plateau (Figure 1). *Stuart et al.* [1985], for example, constrained the average crustal thickness for the Plateau (Figure 1) to be ∼33 km, which closely matches our results of H = 38.2 km and H = 34.9 km for stations CM24 and CM26 respectively (Table 2, Figures 4 and 6b). The same study constrained the crustal thickness beneath the Garoua Rift (Figure 1) to be ∼23 km, a value closely matched by our result of H = 25.3 km at station CM29 (Table 2, Figures 4 and 6b,c). Elevated Vp/Vs ratios here (e.g., 1.84 at CM29) may indicate addition of mafic material to the crust during Cretaceous extension, as is observed in both present-day magma rich [e.g., Ethiopia: *Maguire et al.*, 2006] and non-volcanic rifts [e.g., Baikal: *Thybo and Nielsen*, 2009] worldwide. Additionally, mafic addition to the crust may have occurred more recently at the Adamawa Plateau on the basis of thinned lithosphere [e.g., *Plomerova et al.*, 1993], modestly low mantle seismic wave-speeds [e.g., *Stuart et al.*, 1985; *Dorbath et al.*, 1986; *Reusch et al.*, 2010], and low mantle densities [*Poudjom Djomani et al.*, 1992, 1997; *Nnange et al.*, 2001]. The Afar hotspot is a possible source of low density material, with buoyant asthenosphere flowing laterally beneath continental lithosphere thinned extensively during Mesozoic rifting since the onset of East African hotspot volcanism ∼40 Ma [e.g., *Ebinger and Sleep*, 1998; *Pérez-Gussinyé et al.*, 2009; *Rooney et al.*, 2012a].

Figure 7 shows a summary comparison of crustal thickness constrained in this study for CBSE stations with those of *Tokam et al.* [2010]. Our results are in close agreement with the earlier study, except in instances where the H-κ method was not applicable due to low signal-to-noise ratio P-to-S conversions

(CM01, CM05, CM11, CM13, CM23, CM27: Table 2). At these stations, discrepancies between the results may be due to uncertainties in the Vp/Vs ratio. Alternatively, the data at these stations may not be significantly high quality for use in the detailed 1D modeling employed by *Tokam et al.* [2010].

Towards the continent-ocean transition, in southern Cameroon the crustal thickness of ∼37 km found at stations CM01 and CM05 (Figures 4 and 6c) is somewhat thicker than the 29.9 km value constrained by *Tokam et al.* [2010] and the 26.8 km constrained by the gravity study of *Tadjou et al.* [2009]. The easterly backazimuth of earthquakes used in our study to constrain H at CM01 and CM05 likely means that our study may be sensitive principally to the Congo craton, which lies immediately to the east of these stations (Figure 1).

4.2. Implications for the Crustal Magmatic Plumbing System Beneath the Cameroon Volcanic Line

Present-day melt within the crust would be expected to markedly raise Vp/Vs ratios [>1.9; e.g., *Watanabe*, 1993]; **mafic intrusions emplaced during the CVLs development would, even after cooling, also be expected to raise Vp/Vs ratios compared to the global average value of 1.768, which is dominated by the inherently felsic (low Vp/Vs ratio) shields**. To this end, a striking observation in Figure 5 is that Vp/Vs ratios along portions of the CVL unaffected by Cretaceous rifting (e.g., the Garoua rift) and older magmatic events are markedly low compared to the global mean. Vp/Vs values are, in-fact, more akin to those found in cratons worldwide [e.g., 1.72–1.76 in Archean northern Hudson Bay: *Thompson et al.*, 2010], despite the CVL being a region of active volcanism for ∼30 Ma.

Recent volcanism [ca. 1 Ma; *Halliday et al.*, 1988] at Mount Manengouba (Figure 1) might be expected to have resulted in elevated Vp/Vs ratios at stations CM10 and CM16, but our observations of Vp/Vs ≤ 1.68 indicate that this is not the case. It must be acknowledged that none of the CBSE stations used in this study were located on one of the CVL's active volcanoes. Mount Manengouba, for example, is ∼65 km away from station CM13 (Figure 1). Therefore, we cannot preclude the possibility that melt and mafic magmatic intrusions exist directly beneath the volcanic centres. However, the mean Vp/Vs ratio across the entire study area is 1.74, implying little modification of Precambrian basement has occurred due to the development of the CVL, either by plutonism (e.g., gabbroic intrusions) or by the emplacement of mafic cumulates due to fractionation of magmas in the crust prior to eruption. This is in slight contrast to *Tokam et al.* [2010], who cite seismological data as evidence for thin, shallow crustal intrusions beneath the CBSE network. Our low Vp/Vs ratios show that if these bodies exist, they are not volumetrically significant enough to affect our bulk crustal results. Our results thus agree instead with petrological studies that **attribute low volume, high pressure magmas to melting of sub-continental lithospheric mantle that has experienced only small amounts of crustal fractionation** [e.g., *Fitton and Dunlop*, 1985; *Halliday et al.*, 1988; *Marzoli et al.*, 2000; *Suh et al.*, 2003; *Déruelle et al.*, 2007; *Yokoyama et al.*, 2007]. Such low-volume, high-pressure magmas are expected to form within the sub-continental lithospheric mantle and exhibit relatively little fractionation within the crust [e.g., *Suh et al.*, 2003].

The presence of melt beneath the Moho can sometimes lead to magmatic addition to the base of the crust (often termed underplate). Underplate has anomalously fast seismic velocities when compared to unaltered crust, but anomalously slow seismic velocities when compared to the mantle [e.g., *Maguire et al.*, 2006]. Receiver function H-κ analysis is sometimes sensitive to the top, not the bottom, of such layers [e.g., *Stuart et al.*, 2006], which can nevertheless still be detected via crustal receiver function analysis. The amplitude of the Ps arrival and, in particular, subsequent reverberent phases (PpPs and PpSs+PsPs) are highly sensitive to the sharpness of the velocity discontinuity that produces them [e.g., *Zheng et al.*, 2008]. This is illustrated in Figure 8: note the lower amplitude arrivals in the underplate example, where the transition from 6.5 kms^{-1} crust to 8 kms^{-1} mantle occurs gradually, not abruptly.

Figure 9 shows a comparison of single station stacks for station CM04 on the Congo Craton, CM26 on the CVL, and CM29 in the Garoua Rift. In each case, the Ps arrival and subsequent reverberent phases are sharp, indicating an abrupt transition from relatively felsic lower crust to peridotitic mantle. Nowhere in the study area do we find evidence for thick magmatic underplate/lower-crustal intrusions.

When considered in light of the petrological literature, our low Vp/Vs ratio observations and sharp Moho P-to-S conversions suggest strongly that the protracted magmatic activity along the CVL has resulted in very little compositional modification of the felsic Precambrian basement rocks. The CVL's alkali basaltic melts, sourced from sub-crustal depths, are probably therefore transported quickly to the surface such that little shallow fractionation can occur. High strain rates associated with this rapid movement of magma are capable of generating seismicity in the lithospheric mantle [e.g., Hawaii: *Okubo and Wolfe*, 2008], where temperatures should be too high for brittle failure to occur [*McKenzie et al.*, 2005]. Accordingly, sub-continental lithospheric mantle (∼55-60 km depth) earthquakes have been observed beneath Mount Cameroon prior to its recent eruptions [*Tabod et al.*, 1992; *Ateba and Ntepe*, 1997; *Ateba et al.*, 2009], which may be the result of the aforementioned high strain rates.

4.3. Comparisons with Other Hotspots and Implications for the Upper Mantle Beneath the Cameroon Volcanic Line

Comparisons with rifts and other hotspots highlights the uniqueness of bulk crustal properties of the CVL (Table 3). The average Vp/Vs ratios of the other hotspots and rifts are all above the global average of 1.768 [*Christensen*, 1996]. Thus, explanations for CVL development based on observations at other hotspots worldwide are not straightforward.

The case for present-day melt within the crust is well established at many hotspots and rifts. In Iceland and Hawaii, for example, ongoing volcanic eruptions provide clear evidence for the melt migration required to maintain melt within the crust for periods of more than a few thousand years [e.g., *McKenzie*, 1984; *Rose and Brenan*, 2001]. The Ethiopian rift in East Africa, magmatically active for around the same period of time as the CVL (∼30 Ma), is an excellent venue to compare and contrast styles of magmatism with those we observe Cameroon. Magnetotelluric studies image present-day melt beneath the Ethiopian rift [*Whaler and Hautot*, 2006], while geodetic studies provide evidence in support of ongoing crustal melt migration, even in the absence of historical volcanism [*Biggs et al.*, 2011; *Keir et al.*, 2011]. These crustal properties result in bulk crustal Vp/Vs ratios in Ethiopia of up to ∼2, which is difficult to explain without invoking a hypothesis of melt within the crust [e.g., *Stuart et al.*, 2006].

In addition to present-day melt within the crust in Ethiopia, recent geophysical studies have found evidence for seismically fast [e.g., *Maguire et al.*, 2006; *Daly et al.*, 2008], dense [*Cornwell et al.*, 2006; *Mickus et al.*, 2007], cooled gabbroic intrusions that are believed to have have accommodated ∼80% of extension in the Ethiopian rift since Quaternary times [e.g., *Ebinger and Casey*, 2001]. Petrological data also indicate extensive fractionation and modification of the crust and mantle lithosphere beneath the Ethiopian rift [e.g., *Rooney et al.*, 2005, 2011]. Further south in the EAR, seismic and gravity data from Kenya provide evidence for magma intrusion into the Pan African Mozambique belt [e.g., *Simiyu and Keller*, 2001]. **Ongoing dike intrusion has been identified geodetically via InSAR study [*Biggs et al.*, 2009]. Underplating/magmatic addition to the lower crust has been detected seismically beneath the uplifted Ethiopia Plateau [e.g., *Maguire et al.*, 2006], as well as in Hawaii [*Darbyshire et al.*, 2000] and Iceland [*Leahy et al.*, 2010]. In receiver function data such layers are manifest as gradational velocity profiles at Moho depths, as illustrated in Figure 8, but distinct from that which we observe beneath the CVL (Figure 9).**

In contrast to the aforementioned hotspots and rifts, the Vp/Vs ratios observed along the CVL are low compared to the global average, indicating a bulk crustal composition of mainly granodiorite and granite-gneiss [e.g., *Christensen*, 1996], with no requirement for present-day melt or significant volumes of intruded mafic material. In support of this, geophysical evidence for magmatic intrusion along the CVL is limited. While *Poudjom Djomani et al.* [1997], suggest tentatively that gravity data across the Adamawa plateau can be explained in part by magma crustal intrusions, residual Bouguer gravity maps for the CVL as a whole [e.g., *Fairhead and Okereke*, 1987], present no evidence for dense mafic intrusions beneath the CVL, consistent with our hypothesis of a relatively unmodified CVL crust. **Instead, the principal reason for the plateau uplift is thus more likely a modestly buoyant mantle. Evidence in support of this view includes observations of lower mantle seismic wave-speeds compared to the surrounding area [e.g., *Dorbath et al.*, 1986; *Reusch et al.*, 2010]. Gravity studies also provide evidence for a low density mantle at 70–90 km depth [*Poudjom Djomani et al.*, 1992].**

When reviewed in light of the low bulk crustal Vp/Vs ratios and relatively small volumes of eruptive products, the lack of lower-crustal intrusions in Cameroon indicate that melt generation is lower beneath the CVL than other hotspots and rifts worldwide. This may have the implication that mantle potential temperatures in the region are well below those at rifts and other hotspots. This is consistent with upper**most** mantle P-wave velocities from previous studies of 8 kms^{-1} [*Stuart et al.*, 1985], which are high for a volcanic region when compared to values of 7.4–7.5 kms^{-1} from the Ethiopian Rift [*Bastow and Keir*, 2011], where mantle potential temperature is known to be elevated [e.g., *Rooney et al.*, 2012b]. Alternatively, the volumes of melt due to adiabatic decompression beneath the

CVL [for example, due to shear zone reactivation: e.g., *Fairhead and Binks*, 1991], may simply be negligible compared to regions such as Ethiopia or Iceland, where extensional processes likely contribute significantly to melt production by decompression melting [e.g., *Maguire et al.*, 2006; *Bastow et al.*, 2010]. Either way, hypotheses for the formation and development of the CVL should not likely incorporate large volumes of uppermost mantle melt. Figure 10 illustrates schematically how the melt supply and crustal plumbing system beneath the CVL compares to that in melt-rich settings such as the Ethiopian rift.

5. Conclusions

We have conducted a teleseismic receiver function study of crustal structure in Cameroon to place new constraints on the tectonic subdivisions of the region, and to determine the impact of Cenozoic volcanism on crustal structure along the Cameroon volcanic line.

Within cratonic Cameroon the edge of the Congo Craton, is characterized by an abrupt change in crustal thickness of ∼5 km, which constrains the northern and western edges of the craton to be ∼4°N and ∼10°E respectively, consistent with studies of the Bouguer gravity field.

Consistently low Vp/Vs ratios along the CVL (network average is ∼1.74) indicate strongly that the crust does not presently contain melt; earlier Cenozoic volcanism along the line has also not resulted in the additional of appreciable volumes of mafic material to the lower crust, either as gabbroic intrusions or as the fractionated by-product of alkali volcanism. These observations support previous petrological studies in Cameroon that suggest alkali basaltic magma throughout the CVL has a very short residence time in the crust prior to eruption.

The similarity of P-to-S conversions from beneath the CVL and neighbouring cratonic regions indicates that lower-crustal intrusions (often termed underplate) are not likely present beneath the region. When reviewed in light of the low Vp/Vs ratios across Cameroon, this indicates that hypotheses for the formation of the CVL should not include markedly elevated upper-mantle potential temperatures or large volumes of crustal melt, both of which can explain observations at hotspots and rifts elsewhere. The protracted, yet sporadic development of small-volume alkali melts beneath the CVL may instead be explained better by low melt producing mechanisms such as shear zone reactivation or lithospheric delamination (Figure 10).

6. Figure Captions

Table 1: Age of Volcanism Along the Cameroon Volcanic Line. The timing of the various periods of volcanism north to south along the CVL as described by *Halliday et al.* [1988]. All centers of volcanism show morphological evidence for recent cinder cones with the exception of Principe, Etinde, Bambouto and Mandara Mountains (Figure1).

Table 2: Bulk crustal properties across the CBSE broadband network.

Table 3: A global comparison of global hotspot and rift bulk crustal properties.

Figure 1: Location map of the CBSE seismograph stations (triangles) superimposed on regional topography. Numbers are station codes. The Ntem Complex boundary and the Yaoundé domain boundary are after *Toteu et al.* [2004] respectively. Stars are selected CVL volcanoes. C.A.R.: Central African Republic; CASZ: Central African Shear Zone;

E.G.: Equatorial Guinea. The red areas are regions of Cenozoic volcanism along the CVL taken from *Tokam et al.* [2010].

Figure 2: The global distribution of all the earthquakes used in the study plotted with an azimuthal equidistant map projection. Concentric circles indicate 30° intervals from center of the CBSE network, marked by the triangle. Plate boundaries are black.

Figure 3: Examples of crustal thickness (H) versus Vp/Vs plots from the method of Zhu and Kanamori (2000) and receiver functions for stations CM22 and CM29. On each plot the arrival time of the Moho phase Ps (t1) and subsequent reverberent phases PpPs (t2) and PsPs+PpSs (t3) (determined by Equations 2-4) are marked based on the crustal thickness and Vp/Vs ratios shown in Table 2. The back azimuth for each trace is shown in the top right. The horizontal and vertical lines on the contour plots mark the maximum of the stack defined by Equation 6. The white line is the 2σ error contour.

Figure 4: Variations in crustal thickness (Table 2) across Cameroon determined from receiver function analysis. The thick black lines A-A', B-B', and C-C' show the orientation of transects in Figure 6.

Figure 5: Variations in Vp/Vs ratio across Cameroon determined from receiver function analysis (Table 2). The thick black lines A-A', B-B', and C-C' show the orientation of transects in Figure 6.

Figure 6: Variations in elevation, crustal thickness, and Vp/Vs ratio (a) NW-SE across the southern portion of the CVL and into the Congo Craton; (b) NW-SE across the northern portion of the CVL and the southern tip of the Garoua rift; (c) NE-SW along

the CVL. The dashed line is the average crustal Vp/Vs ratio (1.768). The orientation of the transects is shown on Figures 4 and 5.

Figure 7: A comparison of crustal thickness constrained in this study with that of *Tokam et al.* [2010].

Figure 8: Forward models of receiver functions with (top) and without (bottom) the presence of a high velocity lower-crustal layer. Note the sharpness of the Ps phase and subsequent reverberations when this layer is absent.

Figure 9: Receiver function stacks for stations (a) CM04 on the Congo Craton, (b) CM26 in the CVL, and (c) CM29 in the Garoua Rift, (Figure 1). Note the similarity of shape and amplitude of the Ps and subsequent reverberation phases across the study area. These observations argue against the presence of high-velocity lower-crustal intrusions beneath the CVL (Figure 8).

Figure 10: A summary conceptual cartoon for the magma plumbing system in Cameroon as compared to that in the magmatically active Ethiopian rift. SCLM: sub-continental lithospheric mantle. The Ethiopian sketch is modified after *Rooney et al.* [2011].

Acknowledgments. The seismograms from the CBSE network were sourced from the IRIS DMC. Pennsylvania State University deployed and maintained the CBSE network. We thank Raphael De Plaen, Derek Keir, Jenny Di Leo, Ken Bailey, Luca Caricchi, Tyrone Rooney, Kathy Cashman and Steve Sparks for helpful discussions. Cindy Ebinger and Stewart Fishwick provided helpful reviews that improved markedly the focus of the contribution. IB is funded by the Leverhulme Trust.

References

Ateba, B., and N. Ntepe (1997), Post-Eruptive Seismic Activity of Mount Cameroon (Cameroon), West Africa: a Statistical Analysis, *J. Volcanol. Geotherm. Res.*, *79*(1-2), 25–45.

Ateba, B., C. Dorbath, L. Dorbath, N. Ntepe, M. Frogneux, J. Delmond, and D. Manguelle (2009), Eruptive and earthquake activities related to the 2000 eruption of Mount Cameroon volcano (West Africa), *J. Volcanol. Geotherm. Res.*, *179*(3-4), 206–216, doi:10.1016/j.jvolgeores.2008.11.021.

Basseka, C., Y. Shandini, and J. Tadjou (2011), Subsurface Structural Mapping Using Gravity Data of the Northern Edge of the Congo Craton, South Cameroon, *Geofizika*, *28*(2).

Bastow, I., and D. Keir (2011), The protracted development of the continent-ocean transition in Afar, *Nature Geoscience*, doi: 10.1038/NGEO01095.

Bastow, I., S. Pilidou, J. Kendall, and G. Stuart (2010), Melt-induced seismic anisotropy and magma assisted rifting in Ethiopia: evidence from surface waves, *Geochem. Geophys. Geosyst.*, *11*(Q0AB05), doi:10.1029/2010GC003036.

Biggs, J., E. Anthony, and C. Ebinger (2009), Multiple inflation and deflation events at Kenyan volcanoes, East African Rift, *Geology*, *37*(11), 979–982.

Biggs, J., I. Bastow, D. Keir, and E. Lewi (2011), Pulses of deformation reveal frequently recurring shallow magmatic activity beneath the Main Ethiopian Rift, *Geochem. Geophys. Geosyst.*, doi:10.1029/2011GC003662.

Binks, R., and J. Fairhead (1992), A Plate Tectonic Setting for Mesozoic Rifts of West and Central Africa, *Tectonophysics*, *213*(1-2), 141–151.

Bjarnason, I., and H. Schmeling (2009), The Lithosphere and Asthenosphere of the Iceland Hotspot from Surface Waves, *Geophys. J. Int.*, *178*(1), 394–418.

Browne, S., and J. Fairhead (1983), Gravity Study of the Central African Rift System: A Model of Continental Disruption 1. The Ngaoundere and Abu Gabra Rifts, *Tectonophysics*, *94*(1-4), 187–203.

Burke, K. (2001), Origin of the Cameroon Line of Volcano-Capped Swells, *The Journal of Geology*, pp. 349–362.

Burke, K., and J. Dewey (1973), Plume generated triple junctions: key indicators in applying plate tectonics to old rocks, *Journal of Geology*, *81*, 406–433.

Burke, K., T. Dessauvagie, and A. Whiteman (1971), Opening of the Gulf of Guinea and Geological History of the Benue Depression and Niger Delta, *Nature*, *233*(38), 51–55.

Cahen, L., N. Snelling, J. Delhal, and J. Vail (1984), *The geochronology and evolution of Africa*, 512pp pp., Oxford Univ. Press, New York.

Chen, C. (2002), Variations of Crustal Thickness and Vp/Vs Across Mongolian Foldbelt, the Baikal Rift, and the Siberian Platform: Observations and Interpretation, in *2002 Denver Annual Meeting*.

Christensen, N. (1996), Poisson's ratio and crustal seismology, *J. Geophys. Res.*, *101*(B2), 3139–3156.

Cornwell, D., G. Mackenzie, R. England, P. Maguire, L. Asfaw, and B. Oluma (2006), Northern Main Ethiopian Rift crustal structure from new high-precision gravity data, in The Afar Volcanic Province within the East African Rift System, eds. Yirgu, G. Ebinger, C.J. & Maguire, P.K.H., *Geol. Soc. Lond. Spec. Pub.*, *256*, 307–321.

Daly, E., D. Keir, C. Ebinger, G. Stuart, I. Bastow, and A. Ayele (2008), Crustal tomographic imaging of a transitional continental rift: the Ethiopian rift, *Geophys. J. Int.*, *172*(3), 1033–1048, doi:10.1111/j.1365-246X.2007.03682.x.

Darbyshire, F., I. Bjarnason, R. White, and Ó. Flóvenz (1998), Crustal Structure Above the Iceland Mantle Plume Imaged by the ICEMELT Refraction Profile, *Geophys. J. Int.*, *135*(3), 1131–1149.

Darbyshire, F., R. White, and K. Priestley (2000), Structure of the Crust and Uppermost Mantle of Iceland from a Combined Seismic and Gravity Study, *Earth Planet. Sci. Lett.*, *181*(3), 409–428.

Déruelle, B., I. Ngounouno, and D. Demaiffe (2007), The Cameroon Hot Line (CHL): A Unique Example of Active Alkaline Intraplate Structure in both Oceanic and Continental Lithospheres, *Comptes Rendus Geosciences*, *339*(9), 589–600.

Djomani, Y., J. Nnange, M. Diament, C. Ebinger, and J. Fairhead (1995), Effective Elastic Thickness and Crustal Thickness Variations in West Central Africa Inferred from Gravity Data, *J. Geophys. Res.*, *100*(B11), 22,047–22.

Dorbath, C., L. Dorbath, J. Fairhead, and G. Stuart (1986), A Teleseismic Delay Time Study Across the Central African Shear Zone in the Adamawa Region of Cameroon, West Africa, *Geophys. J. R. Astr. Soc.*, *86*(3), 751–766.

Dugda, M., A. Nyblade, J. Julià, C. Langston, C. Ammon, and S. Simiyu (2005), Crustal structure in Ethiopia and Kenya from receiver function analysis, *J. Geophys. Res.*, *110*(B1), doi:10.1029/2004JB003065.

Durrheim, R., and W. Mooney (1991), Archean and Proterozoic Crustal Evolution: Evidence from Crustal Seismology, *Geology*, *19*(6), 606.

Ebinger, C., and M. Casey (2001), Continental breakup in magmatic provinces: an Ethiopian example, *Geology*, *29*, 527–530.

Ebinger, C., and N. Sleep (1998), Cenozoic magmatism throughout East Africa resulting from impact of a single plume, *Nature*, *395*, 788–791.

Ebinger, C., A. Ayele, D. Keir, J. Rowland, G. Yirgu, T. Wright, M. Belachew, and I. Hamling (2010), Length and timescales of rift faulting and magma intrusion: the Afar rifting cycle from 2005 to present, *Annual Review of Earth and Planetary Sciences*, *38*, 439–466.

Fairhead, J. (1988), Mesozoic Plate Tectonic Reconstructions of the Central South Atlantic Ocean: The Role of the West and Central African Rift System, *Tectonophysics*, *155*(1-4), 181–191.

Fairhead, J., and R. Binks (1991), Differential Opening of the Central and South Atlantic Oceans and the Opening of the West African Rift System, *Tectonophysics*, *187*(1-3), 191–203.

Fairhead, J., and C. Okereke (1987), A Regional Gravity Study of the West African Rift System in Nigeria and Cameroon and its Tectonic Interpretation, *Tectonophysics*, *143* (1-3), 141–159.

Fishwick, S. (2010), Surface Wave Tomography: Imaging of the Lithosphere-Asthenosphere Boundary Beneath Central and Southern Africa?, *Lithos*, *120* (1-2), 63–73.

Fishwick, S., and I. Bastow (2011), Towards a Better Understanding of African Topography, a Review of Passive-Source Seismic Studies of the African Crust and Upper Mantle., in *The Formation and Evolution of Africa: A Synopsis of 3.8 Ga of Earth History*, vol. 357, edited by D. Van Hinsbergen, S. Buiter, T. Torsvik, C. Gaina, and S. Webb, pp. 343–371, Geol. Soc. Lond. Spec. Pubs., doi:10.1144/SP357.19.

Fitton, J. (1980), The Benue Trough and Cameroon Line–a Migrating Rift System in West Africa, *Earth Planet. Sci. Lett.*, *51* (1), 132–138.

Fitton, J. (1987), The cameroon line, west africa: a comparison between oceanic and continental alkaline volcanism, *Geological Society, London, Special Publications*, *30* (1), 273.

Fitton, J., and H. Dunlop (1985), The Cameroon Line, West Africa, and its Bearing on the Origin of Oceanic and Continental Alkali Basalt, *Earth Planet. Sci. Lett.*, *72* (1), 23–38.

Freeth, S. (1979), Deformation of the African Plate as a Consequence of Membrane Stress Domains Generated by Post-Jurassic Drift, *Earth Planet. Sci. Lett.*, *45* (1), 93–104.

Guiraud, R., R. Binks, J. Fairhead, and M. Wilson (1992), Chronology and Geodynamic Setting of Cretaceous-Cenozoic Rifting in West and Central Africa, *Tectonophysics*, *213* (1-2), 227–234.

Halliday, A., A. Dickin, A. Fallick, and J. Fitton (1988), Mantle Dynamics: a Nd, Sr, Pb and O Isotopic Study of the Cameroon Line Volcanic Chain, *J. Petrol.*, *29* (1), 181.

Halliday, A., J. Davidson, P. Holden, C. DeWolf, D. Lee, and J. Fitton (1990), Trace-Element Fractionation in Plumes and the Origin of HIMU Mantle Beneath the Cameroon Line, *Nature*, *347* (6293), 523–528.

Helffrich, G. (2006), Extended-Time Multitaper Frequency Domain Cross-Correlation Receiver-Function Estimation, *Bulletin of the Seismological Society of America*, *96* (1), 344–347.

Keir, D., I. Bastow, K. Whaler, E. Daly, D. Cornwell, and S. Hautot (2009), Lower crustal earthquakes near the Ethiopian rift induced by magmatic processes, *Geochem. Geophys. Geosyst.*, *10*, doi:10.1029/2009GC002382.

Keir, D., C. Pagli, I. Bastow, A. Ayele, and E. Ababa (2011), The magma-assisted removal of Arabia in Afar: Evidence from dike injection in the Ethiopian rift captured using InSAR and seismicity, *Tectonics*, *30* (2), TC2008.

King, S., and D. Anderson (1995), An Alternative Mechanism of Flood Basalt Formation, *Earth Planet. Sci. Lett.*, *136* (3-4), 269–279.

King, S., and D. Anderson (1998), Edge–driven convection, *Earth Planet. Sci. Lett.*, *160*, 289–296.

King, S., and J. Ritsema (2000), African hot spot volcanism: small–scale convection in the upper mantle beneath cratons, *Science*, *290*, 1137–1140.

Langston, C. (1977), The Effect of Planar Dipping Structure on Source and Receiver Responses for Constant Ray Parameter, *Bull., Seis. Soc. Am.*, *67* (4), 1029.

Leahy, G., and J. Park (2005), Hunting for Oceanic Island Moho, *Geophys. J. Int.*, *160* (3), 1020–1026.

Leahy, G., J. Collins, C. Wolfe, G. Laske, and S. Solomon (2010), Underplating of the hawaiian swell: evidence from teleseismic receiver functions, *Geophys. J. Int.*, *183* (1), 313–329.

Lee, D., A. Halliday, J. Fitton, and G. Poli (1994), Isotopic Variations with Distance and Time in the Volcanic Islands of the Cameroon Line: Evidence for a Mantle Plume Origin, *Earth Planet. Sci. Lett.*, *123* (1-3), 119–138.

Maguire, P., G. Keller, S. Klemperer, G. Mackenzie, S. Harder, B. O'Reilly, T. H., L. Asfaw, M. Khan, and M. Amha (2006), Crustal structure of the northern Main Ethiopian Rift from the EAGLE controlled-source survey; a snapshot of incipient lithospheric break-up, in The Afar Volcanic Province within the East African Rift System, eds. Yirgu, G. Ebinger, C.J. & Maguire, P.K.H., *Geol. Soc. Lond. Spec. Pub.*, *259*, 271–293.

Marzoli, A., E. Piccirillo, P. Renne, G. Bellieni, M. Iacumin, J. Nyobe, and A. Tongwa (2000), The Cameroon Volcanic Line Revisited: Petrogenesis of Continental Basaltic Magmas From Lithospheric and Asthenospheric Mantle Sources, *J. Petrol.*, *41* (1), 87–109.

McKenzie, D. (1984), The generation and compaction of partially molten rock, *J. Petrol.*, *25* (3), 713.

McKenzie, D., J. Jackson, and K. Priestley (2005), Thermal structure of oceanic and continental lithosphere, *Earth Planet. Sci. Lett.*, *233* (3-4), 337–349.

Mickus, K., K. Tadesse, G. Keller, and B. Oluma (2007), Gravity analysis of the main Ethiopian rift, *Journal of African Earth Sciences*, *48* (2-3), 59–69.

Moreau, C., J. Regnoult, B. Déruelle, and B. Robineau (1987), A New Tectonic Model for the Cameroon Line, Central Africa, *Tectonophysics*, *141* (4), 317–334.

Ngako, V., E. Njonfang, et al. (2006), The North-South Paleozoic to Quaternary Trend of Alkaline Magmatism from Niger-Nigeria to Cameroon: Complex Interaction Between Hotspots and Precambrian Faults, *J. Afr. Earth Sci.*, *45* (3), 241–256.

Njonfang, E., A. Nono, P. Kamgang, V. Ngako, and F. Tchoua (2011), Cameroon Line alkaline magmatism (central Africa): A reappraisal, *Geological Society of America Special Papers*, *478*, 173–191.

Nkouathio, D., A. Kagou Dongmo, J. Bardintzeff, P. Wandji, H. Bellon, and A. Pouclet (2008), Evolution of Volcanism in Graben and Horst Structures Along the Cenozoic Cameroon Line (Africa): Implications for Tectonic Evolution and Mantle Source Composition, *Mineralogy and Petrology*, *94* (3), 287–303.

Nnange, J., Y. Djomani, J. Fairhead, and C. Ebinger (2001), Determination of the Isostatic Compensation Mechanism of the Region of the Adamawa Dome, West Central Africa Using the Admittance Technique of Gravity Data., *Afri. J. Sci. Tech.*, *1* (4).

Nzenti, J., P. Barbey, J. Macaudiere, and D. Soba (1988), Origin and Evolution of the Late Precambrian High-Grade Yaounde Gneisses (Cameroon), *Precambrian Research*, *38*(2), 91–109.

Okubo, P., and C. Wolfe (2008), Swarms of similar long-period earthquakes in the mantle beneath Mauna Loa Volcano, *J. Volcanol. Geotherm. Res.*, *178*(4), 787–794.

Oliveira, E., S. Toteu, M. Araújo, M. Carvalho, R. Nascimento, J. Bueno, N. McNaughton, and G. Basilici (2006), Geologic Correlation Between the Neoproterozoic Sergipano Belt (NE Brazil) and the Yaoundé Belt (Cameroon, Africa), *J. Afr. Earth Sci.*, *44*(4-5), 470–478.

Pasyanos, M., and A. Nyblade (2007), A top to bottom lithospheric study of Africa and Arabia, *Tectonophysics*, *444*(1-4), 27–44.

Pérez-Gussinyé, M., M. Metois, M. Fernández, J. Vergés, J. Fullea, and A. Lowry (2009), Effective elastic thickness of Africa and its relationship to other proxies for lithospheric structure and surface tectonics, *Earth Planet. Sci. Lett.*, *287*(1-2), 152–167.

Plomerova, J., V. Babuška, C. Dorbath, L. Dorbath, and R. Lillie (1993), Deep Lithospheric Structure Across the Central African Shear Zone in Cameroon, *Geophys. J. Int.*, *115*(2), 381–390.

Poudjom Djomani, Y., M. Diament, and Y. Albouy (1992), Mechanical Behaviour of the Lithosphere Beneath the Adamawa Uplift (Cameroon, West Africa) Based on Gravity Data, *J. Afr. Earth Sci.*, *15*(1), 81–90.

Poudjom Djomani, Y., M. Diament, and M. Wilson (1997), Lithospheric Structure Across the Adamawa Plateau (Cameroon) from Gravity Studies, *Tectonophysics*, *273*(3-4), 317–327.

Priestley, K., D. McKenzie, E. Debayle, and S. Pilidou (2008), The African upper mantle and its relationship to tectonics and surface geology, *Geophys. J. Int.*, *175*(3), 1108–1126.

Rankenburg, K., J. Lassiter, and G. Brey (2005), The Role of Continental Crust and Lithospheric Mantle in the Genesis of Cameroon Volcanic Line Lavas: Constraints from Isotopic Variations in Lavas and Megacrysts from the Biu and Jos Plateaux, *J. Petrol.*, *46*(1), 169.

Reusch, A., A. Nyblade, D. Wiens, P. Shore, B. Ateba, C. Tabod, and J. Nnange (2010), Upper mantle structure beneath Cameroon from body wave tomography and the origin of the Cameroon Volcanic Line, *Geochem. Geophys. Geosyst.*, *11*(10), Q10W07.

Rooney, T., T. Furman, G. Yirgu, and D. Ayalew (2005), Structure of the Ethiopian lithosphere: Xenolith evidence in the Main Ethiopian Rift, *Geochemica et Cosmochimica Acta*, *69*(15), 3889–3910, doi:10.1016/j.gca.2005.03.043.

Rooney, T., I. Bastow, and D. Keir (2011), Insights into extensional processes during magma assisted rifting: Evidence from aligned scoria cones, *J. Volcanol. Geotherm. Res.*, pp. 83–96, doi:10.1016/j.jvolgeores.2010.07.019.

Rooney, T., B. Hanan, D. Graham, T. Furman, J. Blichert-Toft, and J. Schilling (2012a), Upper Mantle Pollution during Afar Plume–Continental Rift Interaction, *J. Petrol.*, *53*(2), 365–389.

Rooney, T., C. Herzberg, and I. Bastow (2012b), Elevated mantle temperature beneath East Africa, *Geology*, *40*(G32382R1), 27–40, doi:10.1130/G32382.1.

Rose, L., and J. Brenan (2001), Wetting properties of Fe-Ni-Co-Cu-OS melts against olivine: Implications for sulfide melt mobility, *Economic Geology*, *96*(1), 145.

Schimmel, M., and H. Paulssen (1997), Noise reduction and detection of weak, coherent signal through phase-weighted stacks, *Geophys. J. Int.*, *130*, 497–505.

Schutt, D., K. Dueker, and H. Yuan (2008), Crust and Upper Mantle Velocity Structure of the Yellowstone Hot Spot and Surroundings, *J. Geophys. Res.*, *113*.

Shandini, Y., J. Tadjou, C. Tabod, and J. Fairhead (2010), Gravity Data Interpretation in the Northern Edge of the Congo Craton, South-Cameroon, *Anuário do Instituto de Geociências*, *33*(1), 73–82.

Silveira, G., L. Vinnik, E. Stutzmann, V. Farra, S. Kiselev, and I. Morais (2010), Stratification of the Earth Beneath the Azores from P and S Receiver Functions, *Earth Planet. Sci. Lett.*, *299*, 91–103.

Simiyu, S., and G. Keller (2001), An integrated geophysical analysis of the upper crust of the southern Kenya rift, *Geophys. J. Int.*, *147*, 543–561.

Stachnik, J., K. Dueker, D. Schutt, and H. Yuan (2008), Imaging Yellowstone Plume-Lithosphere Interactions from Inversion of Ballistic and Diffusive Rayleigh wave Dispersion and Crustal Thickness data, *Geochem. Geophys. Geosyst.*, *9*(6).

Stuart, G., J. Fairhead, L. Dorbath, and C. Dorbath (1985), Crustal Structure of the Adamawa Plateau Cameroon, *Science and Technology Review*, *1*(1-2), 25–35.

Stuart, G., I. Bastow, and C. Ebinger (2006), Crustal structure of the northern Main Ethiopian rift from receiver function studies, in The Afar Volcanic Province within the East African Rift System, eds. Yirgu, G. Ebinger, C.J. & Maguire, P.K.H., *Geol. Soc. Lond. Spec. Pub.*, *259*, 271–293.

Suh, C., S. Ayonghe, R. Sparks, C. Annen, J. Fitton, R. Nana, and A. Luckman (2003), The 1999 and 2000 Eruptions of Mount Cameroon: Eruption Behaviour and Petrochemistry of Lava, *Bulletin of volcanology*, *65*(4), 267–281.

Tabod, C., J. Fairhead, G. Stuart, B. Ateba, and N. Ntepe (1992), Seismicity of the Cameroon Volcanic Line, 1982-1990, *Tectonophysics*, *212*(3-4), 303–320.

Tadjou, J., R. Nouayou, J. Kamguia, H. Kande, and E. Manguelle-Dicoum (2009), Gravity Analysis of the Boundary Between the Congo Craton and the Pan-African Belt of Cameroon, *Austrian J. Earth Sci*, *102*(1), 71–79.

Tchameni, R., K. Mezger, N. Nsifa, and A. Pouclet (2000), Neoarchćan Crustal Evolution in the Congo Craton: Evidence From K Rich Granitoids of the Ntem Complex, Southern Cameroon, *J. Afr. Earth Sci.*, *30*(1), 133–147.

Tchameni, R., K. Mezger, N. Nsifa, and A. Pouclet (2001), Crustal Origin of Early Proterozoic Syenites in the Congo Craton (Ntem Complex), South Cameroon, *Lithos*, *57*(1), 23–42.

Tedla, G., M. Meijde, A. Nyblade, and F. Meer (2011), A Crustal Thickness map of Africa Derived From a Global Gravity Field Model Using Euler Deconvolution, *Geophys. J. Int.*

Teitchou, M., M. Grégoire, R. Temdjim, R. Ghogomu, C. Ngwa, and F. Aka (2011), Mineralogical and geochemical fingerprints of mantle metasomatism beneath Nyos volcano (Cameroon volcanic line), *Geological Society of America Special Papers*, *478*, 193–210.

Thompson, D., I. Bastow, G. Helffrich, J. Kendall, J. Wookey, D. Snyder, and D. Eaton (2010), Precambrian crustal evolution: Seismic constraints from the Canadian Shield, *Earth Planet. Sci. Lett.*, *297*, 655–666, doi:10.1016/j.epsl.2010.07.021.

Thybo, H., and C. Nielsen (2009), Magma-compensated crustal thinning in continental rift zones, *Nature*, *457*(7231), 873–876.

Tokam, A., C. Tabod, A. Nyblade, J. Julià, D. Wiens, and M. Pasyanos (2010), Structure of the Crust Beneath Cameroon, West Africa, from the Joint Inversion of Rayleigh Wave Group Velocities and Receiver Functions, *Geophys. J. Int.*, *183*(2), 1061–1076.

Toteu, S., A. Michard, J. Bertrand, and G. Rocci (1987), U/Pb Dating of Precambrian Rocks from Northern Cameroon, Orogenic Evolution and Chronology of the Pan-African Belt of Central Africa, *Precambrian Research*, *37*(1), 71–87.

Toteu, S., W. Van Schmus, J. Penaye, and A. Michard (2001), New U-Pb and Sm-Nd Data from North-Central Cameroon and its Bearing on the pre-Pan African History of Central Africa, *Precambrian Research*, *108*(1-2), 45–73.

Toteu, S., J. Penaye, and Y. Djomani (2004), Geodynamic Evolution of the Pan-African Belt in Central Africa with Special Reference to Cameroon, *Can. J. Earth Sci.*, *41*(1), 73–85.

Watanabe, T. (1993), Effects of water and melt on seismic velocities and their application to characterization of seismic reflectors, *Geophys. Res. Lett.*, *20*, 2933–2936.

Whaler, K., and S. Hautot (2006), The electrical resistivity structure of the crust beneath the northern Ethiopian rift, in The Afar Volcanic Province within the East African Rift System, eds. Yirgu, G. Ebinger, C.J. & Maguire, P.K.H., *Geol. Soc. Lond. Spec. Pub.*, *256*, 293–305.

Wilson, D., R. Aster, J. Ni, S. Grand, M. West, W. Gao, W. Baldridge, and S. Semken (2005), Imaging the Seismic Structure of the Crust and Upper Mantle Beneath the Great Plains, Rio Grande Rift, and Colorado Plateau Using Receiver Functions, *J. Geophys. Res.*, *110*(10.1029).

Yokoyama, T., M. Kusakabe, and E. Nakamura (2007), Plume-Lithosphere Interaction Beneath Mt. Cameroon Volcano, West Africa: Constraints From 238U-230Th-226Ra and Sr-Nd-Pb Isotope Systematics, *Geochimica et Cosmochimica Acta*, *71*(7), 1835–1854.

Zheng, T., L. Zhao, W. Xu, and R. Zhu (2008), Insight into modification of North China Craton from seismological study in the Shandong Province, *Geophys. Res. Lett.*, *35*(22), L22,305.

Zhu, L., and H. Kanamori (2000), Moho depth variation in southern California from teleseismic receiver functions, *J. Geophys. Res.*, *105*(B2), 2969–2980.

Sample	**Age (Ma)**
Biu Plateau	<5
Manadara Mountains	30
Adamawa Plateau	8
Oku	22
Bambouto	18
Manengouba	1
Mount Cameroon	0
Etinde	<0.5
Bioko	0
Principe	3.5, 6, 21, 31
Sao Tome	0, 3, 6.4, 7.4
Pagalu (Annobon)	5

Table 1. Age of Volcanism Along the Cameroon Volcanic Line. The timing of the various periods of volcanism north to south along the CVL as described by *Halliday et al.* [1988]. All centers of volcanism show morphological evidence for recent cinder cones with the exception of Principe, Etinde, Bambouto and Mandara Mountains (Figure 1)

Stations (Figure 1)	N	H_{PWS} (km) (Figure 4)	δH_{PWS} (km)	κ_{PWS}	$\delta\kappa_{PWS}$	H_{lin} (km)	δH_{lin} (km)	κ_{lin}	$\delta\kappa_{lin}$
CM02	3	44.6	0.6	1.71	0.02	44.2	1.3	1.70	0.04
CM03	5	44.6	0.7	1.65	0.03	44.6	1.0	1.66	0.03
CM04	4	47.5	1.0	1.78	0.05	47.5	1.2	1.76	0.05
CM06	7	41.8	0.7	1.82	0.04	41.0	1.0	1.87	0.05
CM07	12	41.8	0.7	1.73	0.03	41.4	1.1	1.74	0.04
CM10	6	35.8	0.7	1.68	0.04	35.4	1.1	1.72	0.06
CM12	5	37.8	0.7	1.73	0.03	37.4	1.2	1.73	0.05
CM16	4	34.1	0.6	1.67	0.03	34.1	1.2	1.68	0.05
CM17	5	37.8	0.9	1.66	0.04	37.0	1.3	1.69	0.05
CM20	3	33.7	0.6	1.84	0.04	33.7	1.0	1.86	0.06
CM21	6	34.1	0.7	1.76	0.04	34.1	1.0	1.76	0.05
CM22	5	35.8	0.6	1.71	0.03	35.4	1.0	1.76	0.06
CM24	13	38.2	0.7	1.68	0.04	37.8	1.0	1.70	0.05
CM25	4	38.2	0.6	1.74	0.03	37.8	1.1	1.75	0.05
CM26	18	34.9	0.7	1.72	0.04	34.9	1.1	1.71	0.06
CM29	6	25.3	0.8	1.84	0.07	25.3	1.2	1.82	0.09
CM30	4	26.5	0.9	1.75	0.06	26.5	1.2	1.73	0.06
CM32	4	33.3	1.1	1.80	0.08	33.7	1.0	1.74	0.06

Ps picked method

Station	N	H (km)	κ
CM01	6	**37.6**	**1.82**
CM05	**4**	**37.4**	**1.82**
CM11	7	43.3	1.71
CM13	3	36.5	1.68
CM23	10	38.3	1.84
CM27	4	39.0	1.72

Table 2. Bulk crustal properties across the CBSE broadband network.

Hotspot	Vp/Vs	H (km)	Reference
CVL	1.74	∼35	This study.
Hawaii	1.80	10–20	*Leahy and Park* [2005].
Iceland	1.78	20–30	*Darbyshire et al.* [1998]; *Bjarnason and Schmeling* [2009].
Ethiopian Rift	2.00	30–40	*Stuart et al.* [2006].
Azores	1.80–1.90	20–30	*Silveira et al.* [2010].
Yellowstone	1.76–1.87	38–54	*Schutt et al.* [2008]; *Stachnik et al.* [2008].
S. EAR	1.84	38–42	*Dugda et al.* [2005].
Baikal	1.82	45	*Chen* [2002].
Rio Grande	1.78	35	*Wilson et al.* [2005].

Table 3. A global comparison of global hotspot and rift bulk crustal properties.

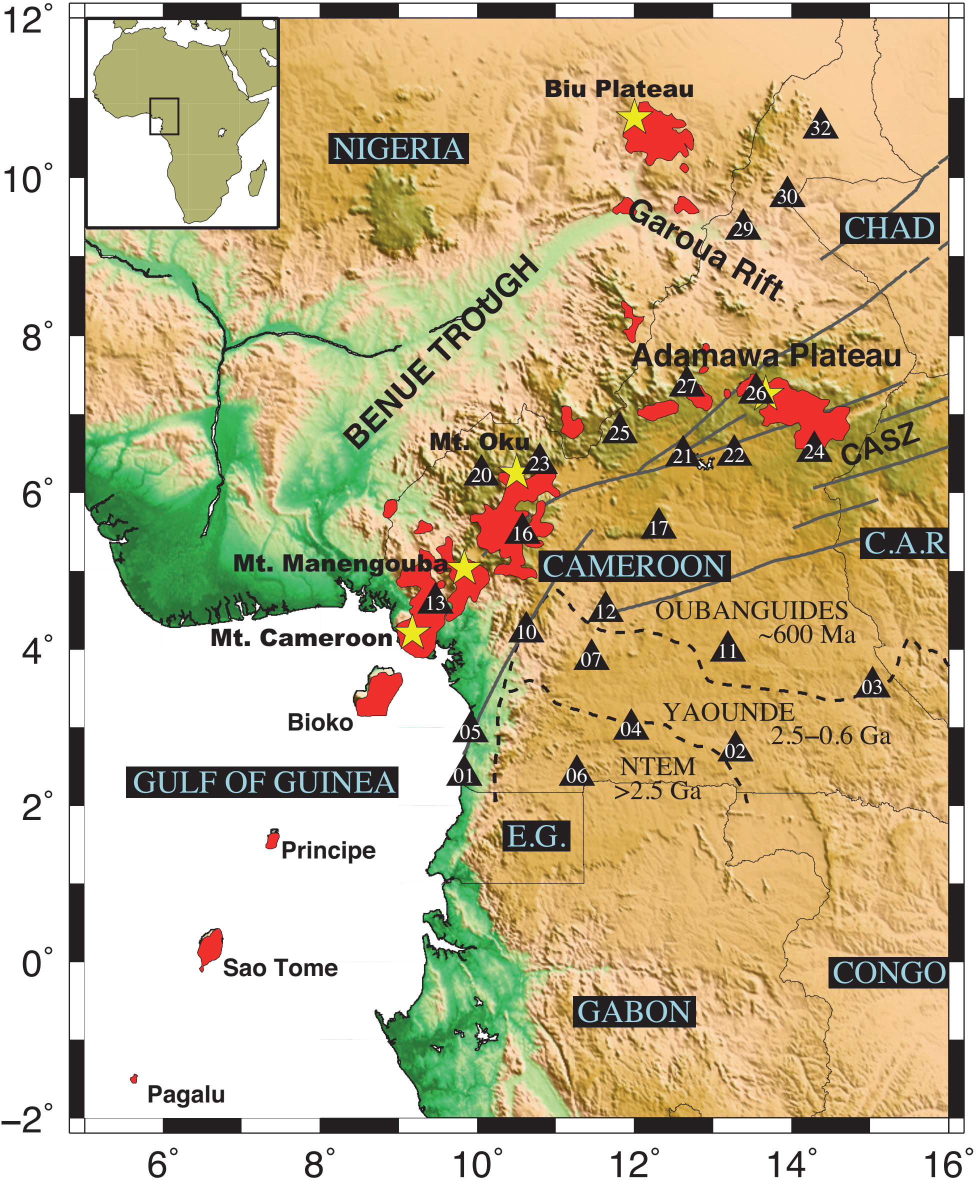

Biu Plateau
NIGERIA
CHAD
Garoua Rift
BENUE TROUGH
Adamawa Plateau
CASZ
Mt. Oku
Mt. Manengouba
Mt. Cameroon
CAMEROON
C.A.R
OUBANGUIDES
~600 Ma
YAOUNDE
2.5–0.6 Ga
NTEM
>2.5 Ga
Bioko
GULF OF GUINEA
E.G.
Principe
Sao Tome
CONGO
GABON
Pagalu
01
02
03
04
05
06
07
10
11
12
13
16
17
20
21
22
23
24
25
26
27
29
30
32
12°
10°
8°
6°
4°
2°
0°
−2°
6°
8°
10°
12°
14°
16°

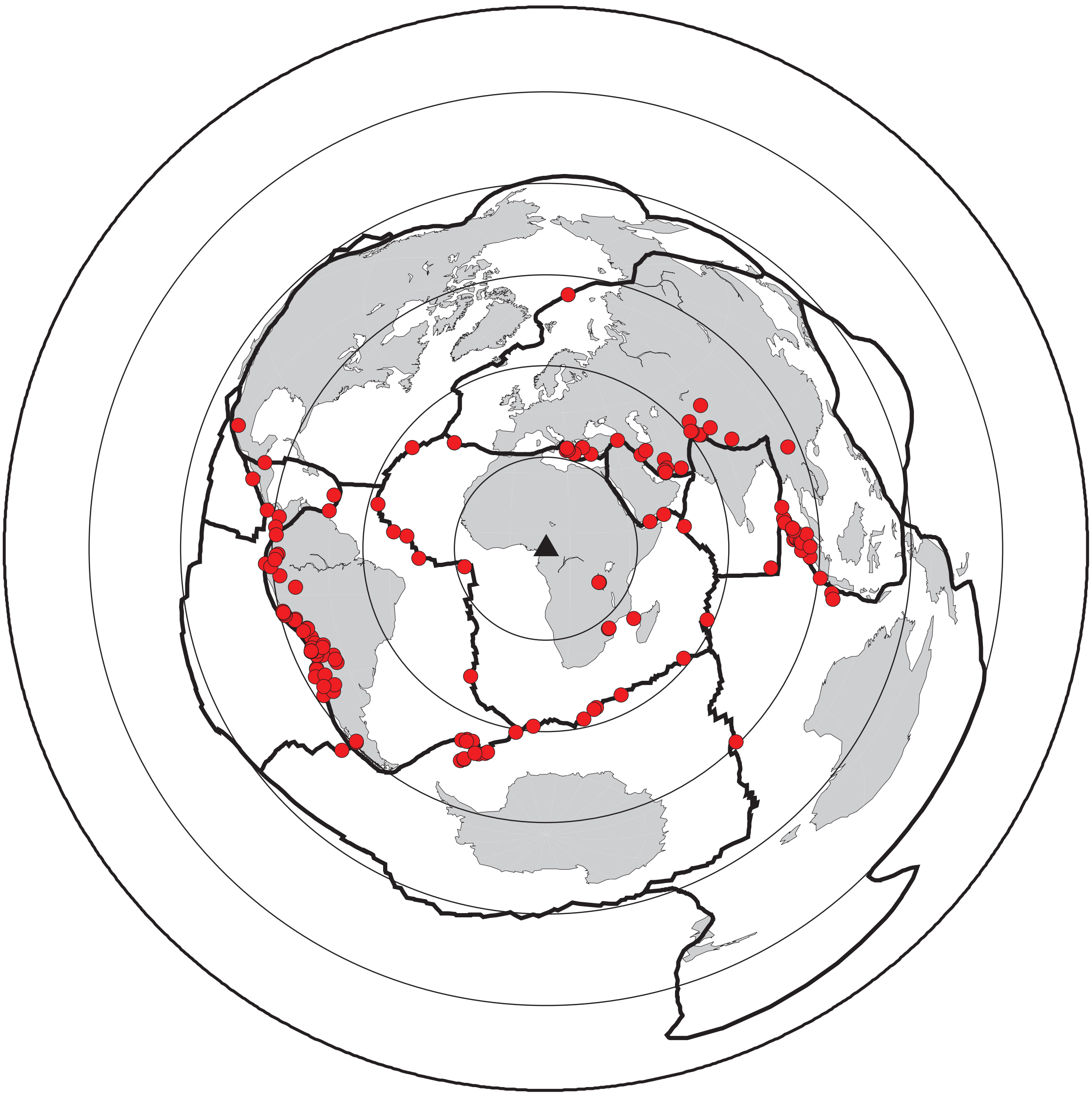

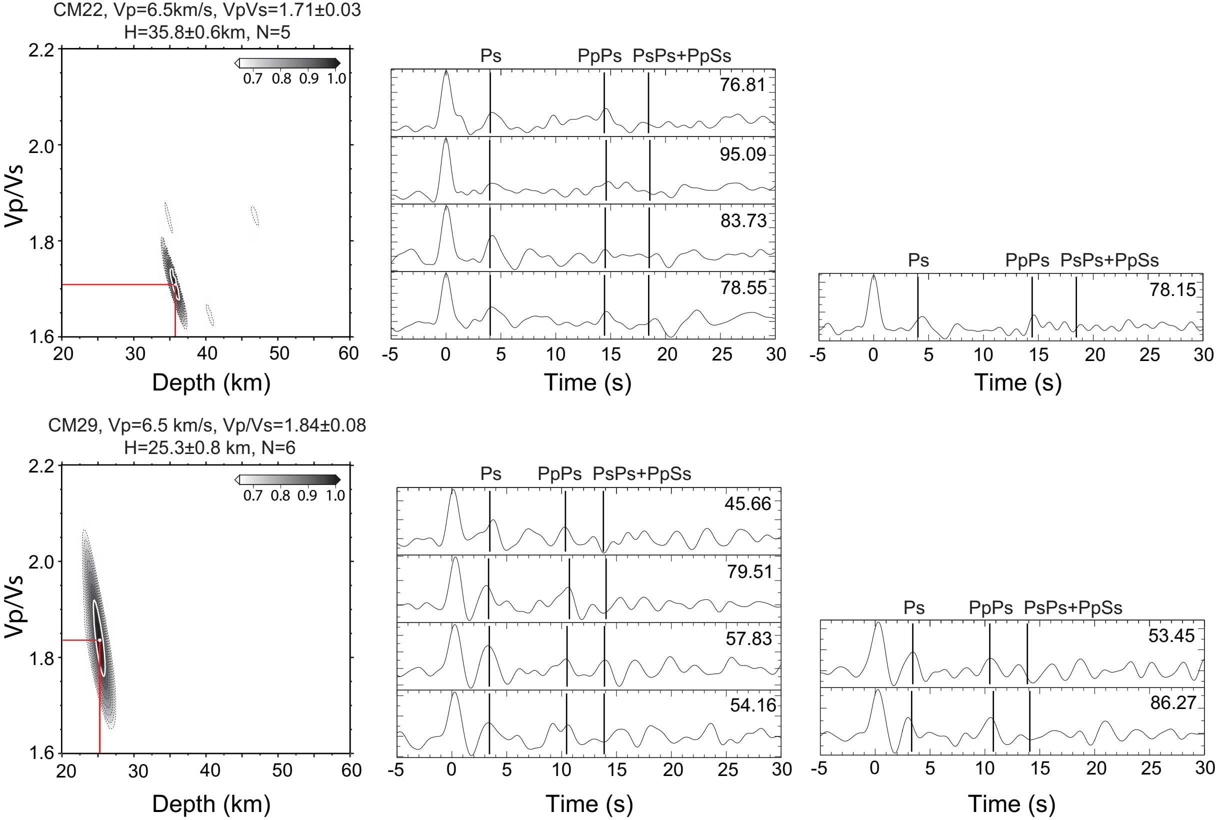
CM22, Vp=6.5km/s, VpVs=1.71±0.03
H=35.8±0.6km, N=5
Vp/Vs
Depth (km)
0.7 0.8 0.9 1.0
Ps
PpPs
PsPs+PpSs
76.81
95.09
83.73
78.55
78.15
Time (s)
CM29, Vp=6.5 km/s, Vp/Vs=1.84±0.08
H=25.3±0.8 km, N=6
45.66
79.51
57.83
54.16
53.45
86.27

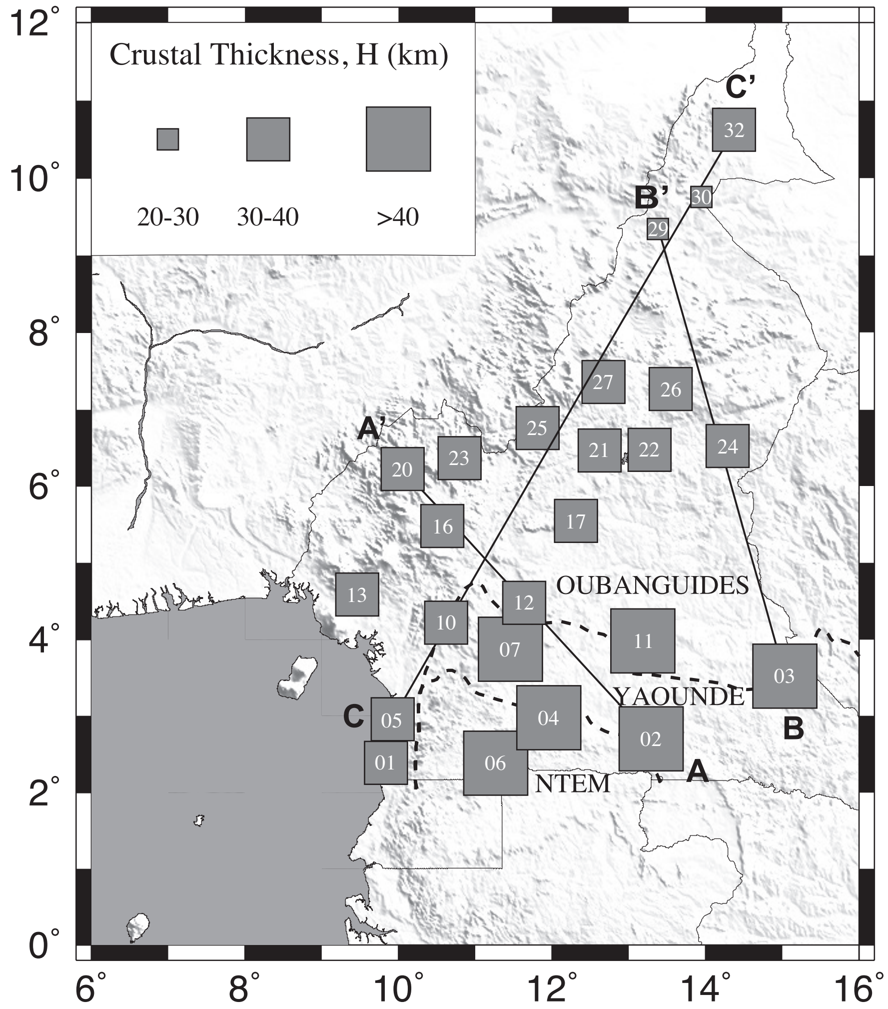

Crustal Thickness, H (km)
20-30
30-40
>40
12°
10°
8°
6°
4°
2°
0°
6°
8°
10°
12°
14°
16°
C'
32
B'
30
29
27
26
25
21
22
24
A'
20
23
16
17
OUBANGUIDES
13
12
10
07
11
03
YAOUNDE
C
05
04
B
02
01
06
A
NTEM

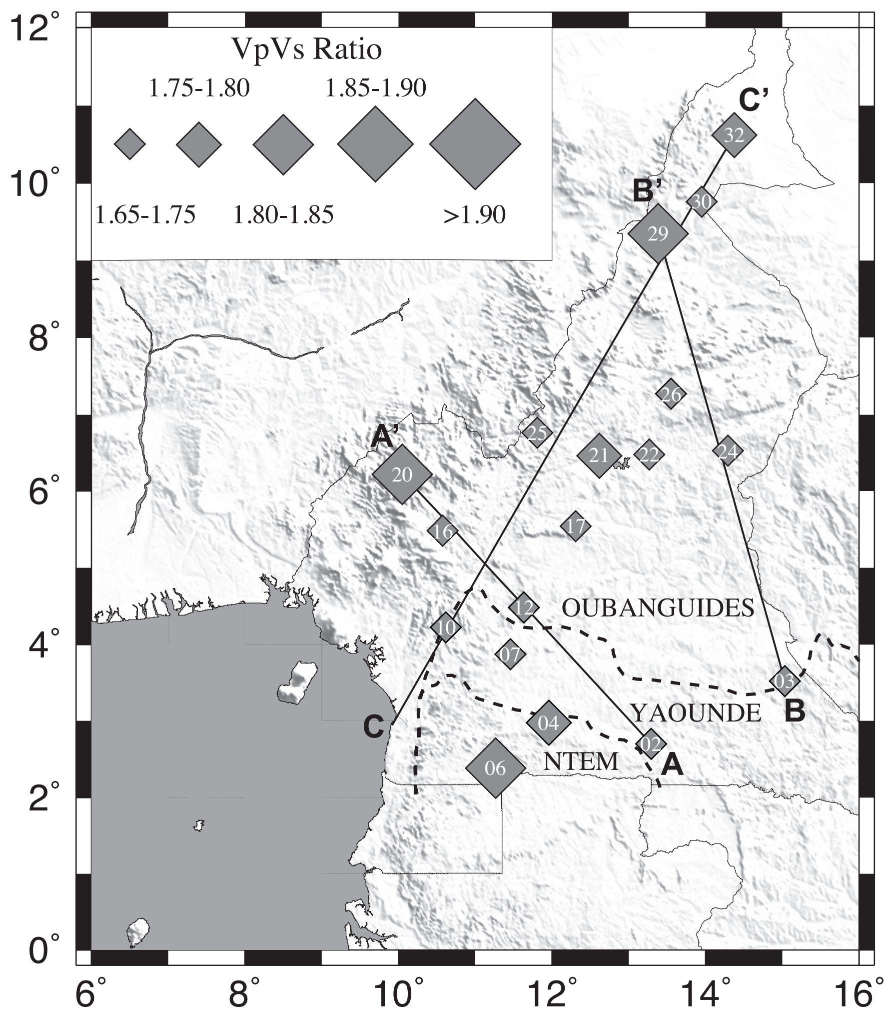

VpVs Ratio
1.75-1.80
1.85-1.90
1.65-1.75
1.80-1.85
>1.90
C'
B'
A'
32
30
29
26
25
21
22
24
20
16
17
12
10
07
04
02
06
03
OUBANGUIDES
YAOUNDE
NTEM
C
B
A
12°
10°
8°
6°
4°
2°
0°
6°
8°
10°
12°
14°
16°

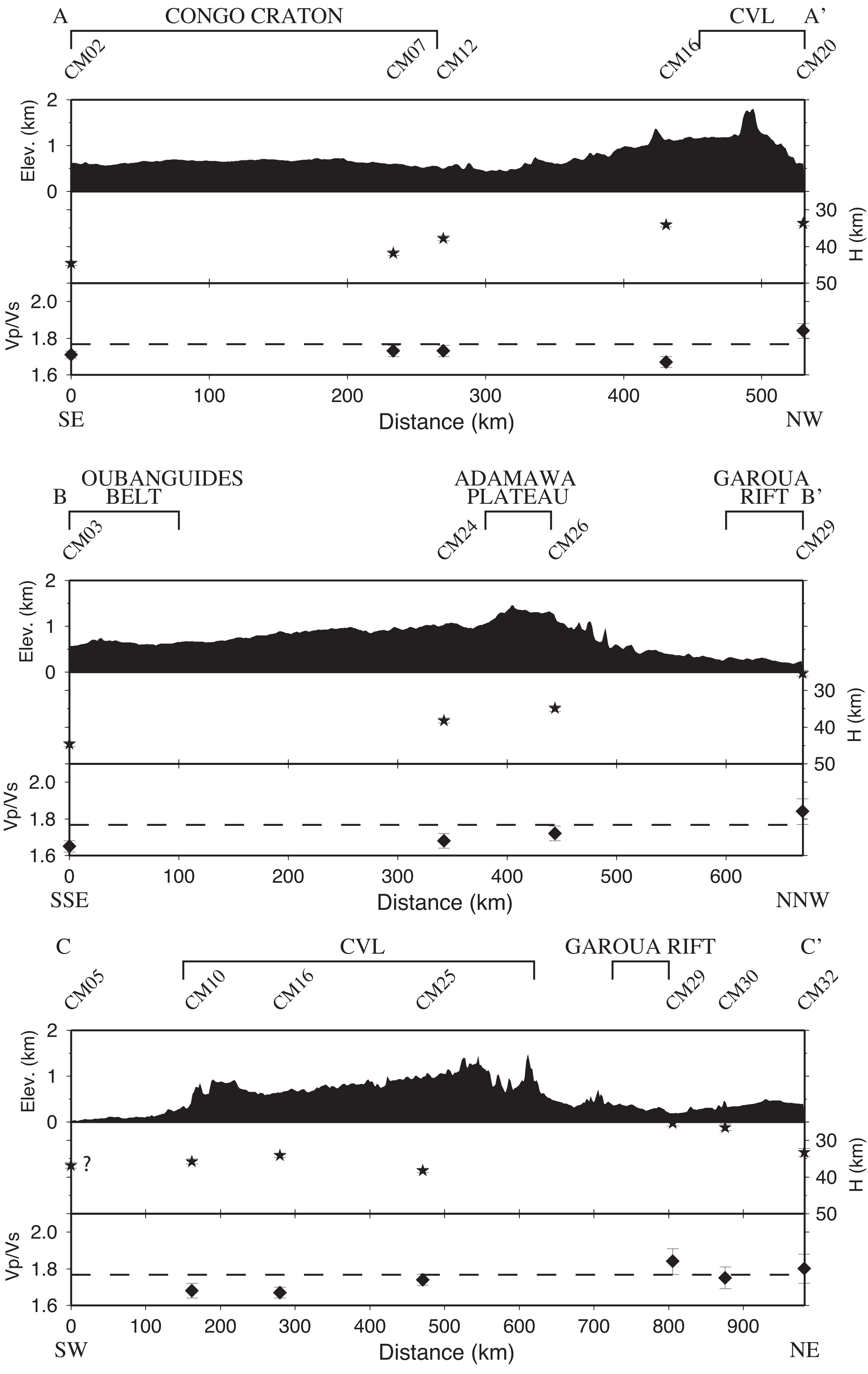

A
CONGO CRATON
CVL
A'
CM02
CM07
CM12
CM16
CM20
Elev. (km)
H (km)
Vp/Vs
Distance (km)
SE
NW
B
OUBANGUIDES
BELT
ADAMAWA
PLATEAU
GAROUA
RIFT
B'
CM03
CM24
CM26
CM29
SSE
NNW
C
CVL
GAROUA RIFT
C'
CM05
CM10
CM16
CM25
CM29
CM30
CM32
?
SW
NE

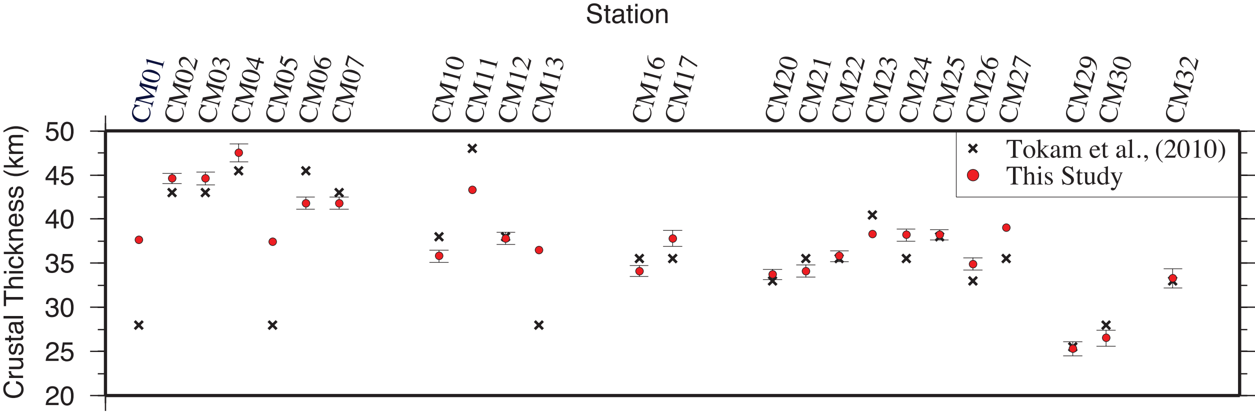

Station
CM01
CM02
CM03
CM04
CM05
CM06
CM07
CM10
CM11
CM12
CM13
CM16
CM17
CM20
CM21
CM22
CM23
CM24
CM25
CM26
CM27
CM29
CM30
CM32
Crustal Thickness (km)
50
45
40
35
30
25
20
Tokam et al., (2010)
This Study

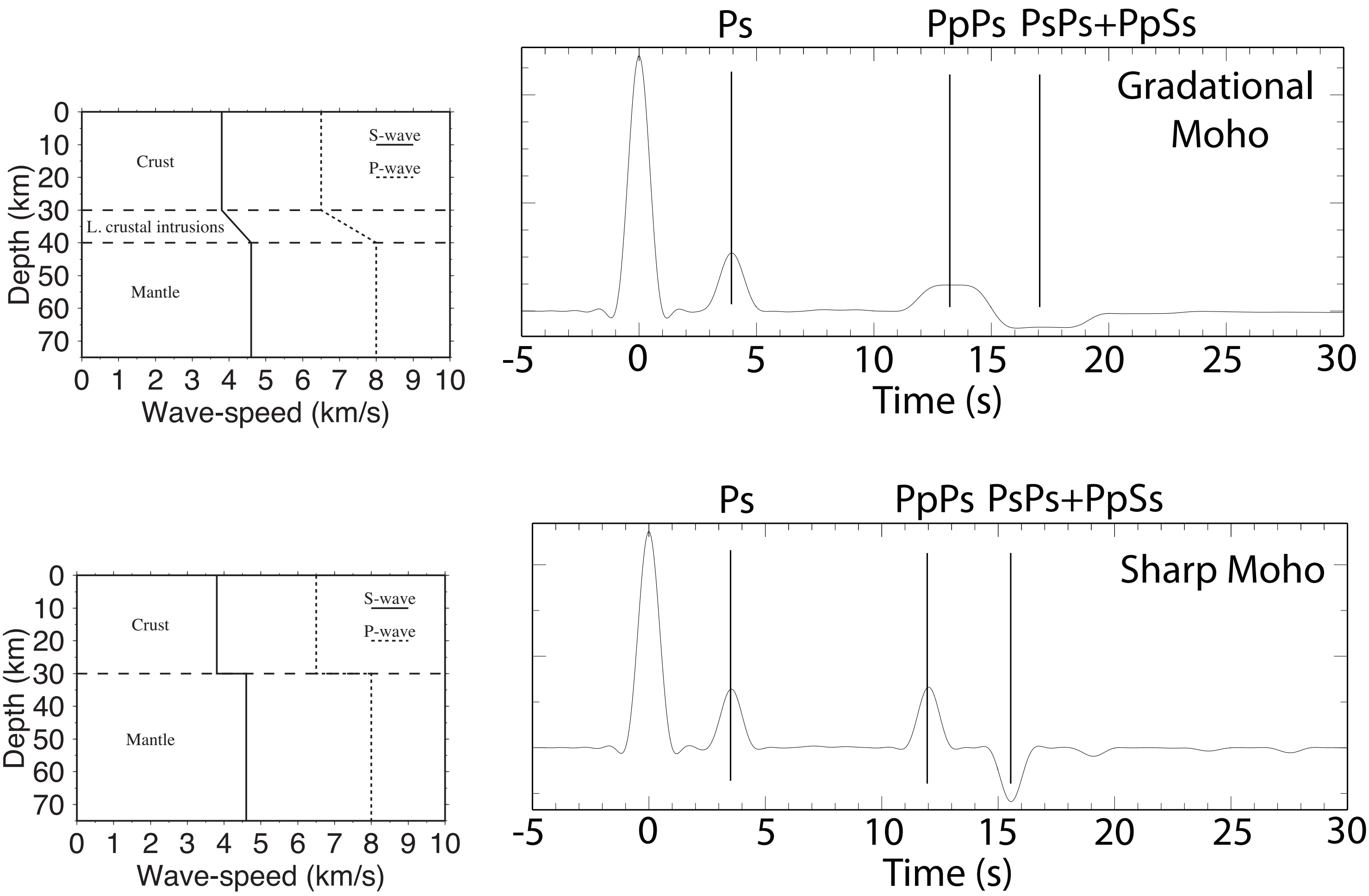
Ps
PpPs
PsPs+PpSs
Gradational Moho
Time (s)
Depth (km)
Wave-speed (km/s)
Crust
L. crustal intrusions
Mantle
S-wave
P-wave
Sharp Moho

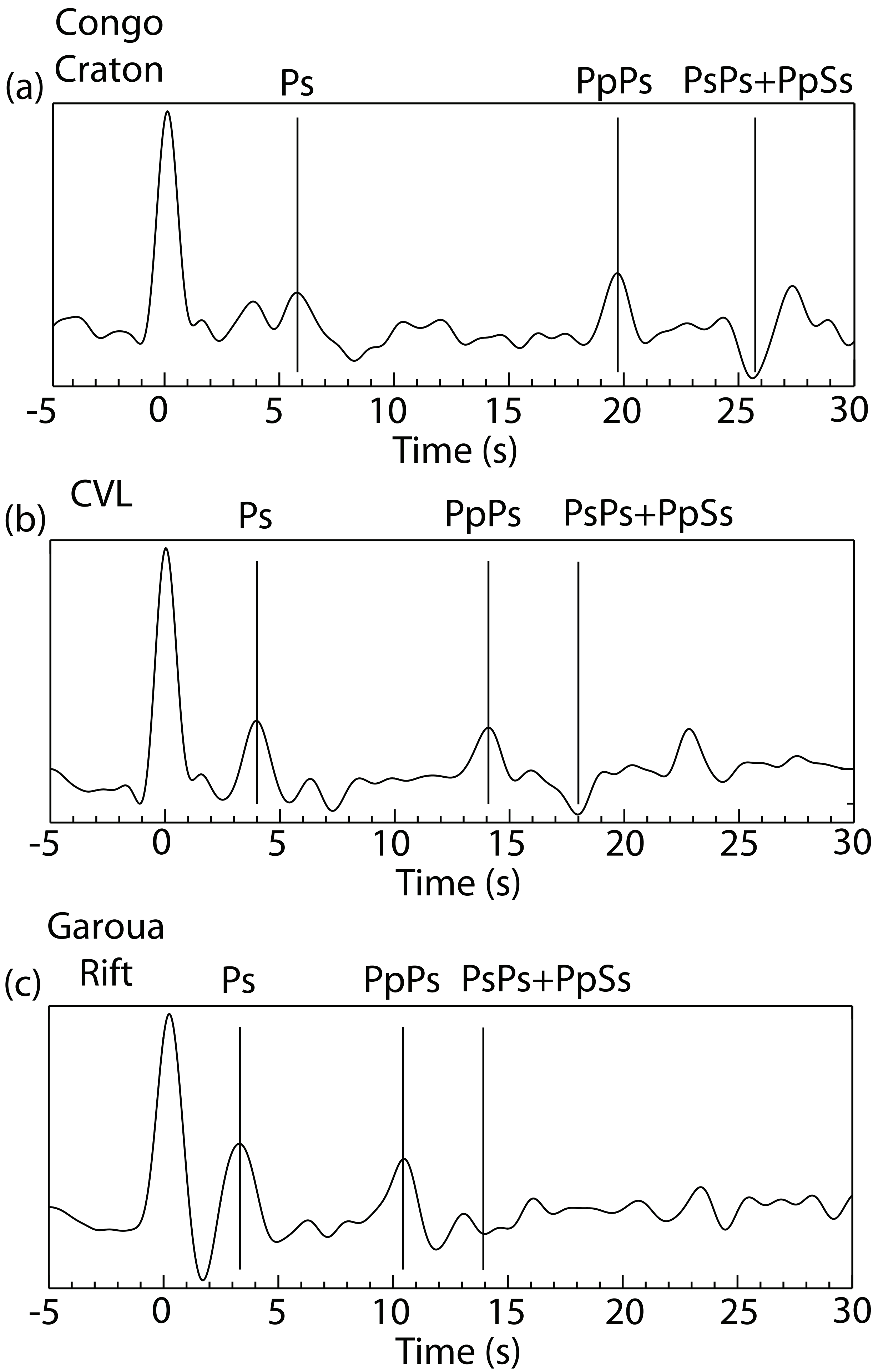
Congo
Craton
(a)
Ps
PpPs
PsPs+PpSs
-5
0
5
10
15
20
25
30
Time (s)
CVL
(b)
Ps
PpPs
PsPs+PpSs
-5
0
5
10
15
20
25
30
Time (s)
Garoua
Rift
(c)
Ps
PpPs
PsPs+PpSs
-5
0
5
10
15
20
25
30
Time (s)

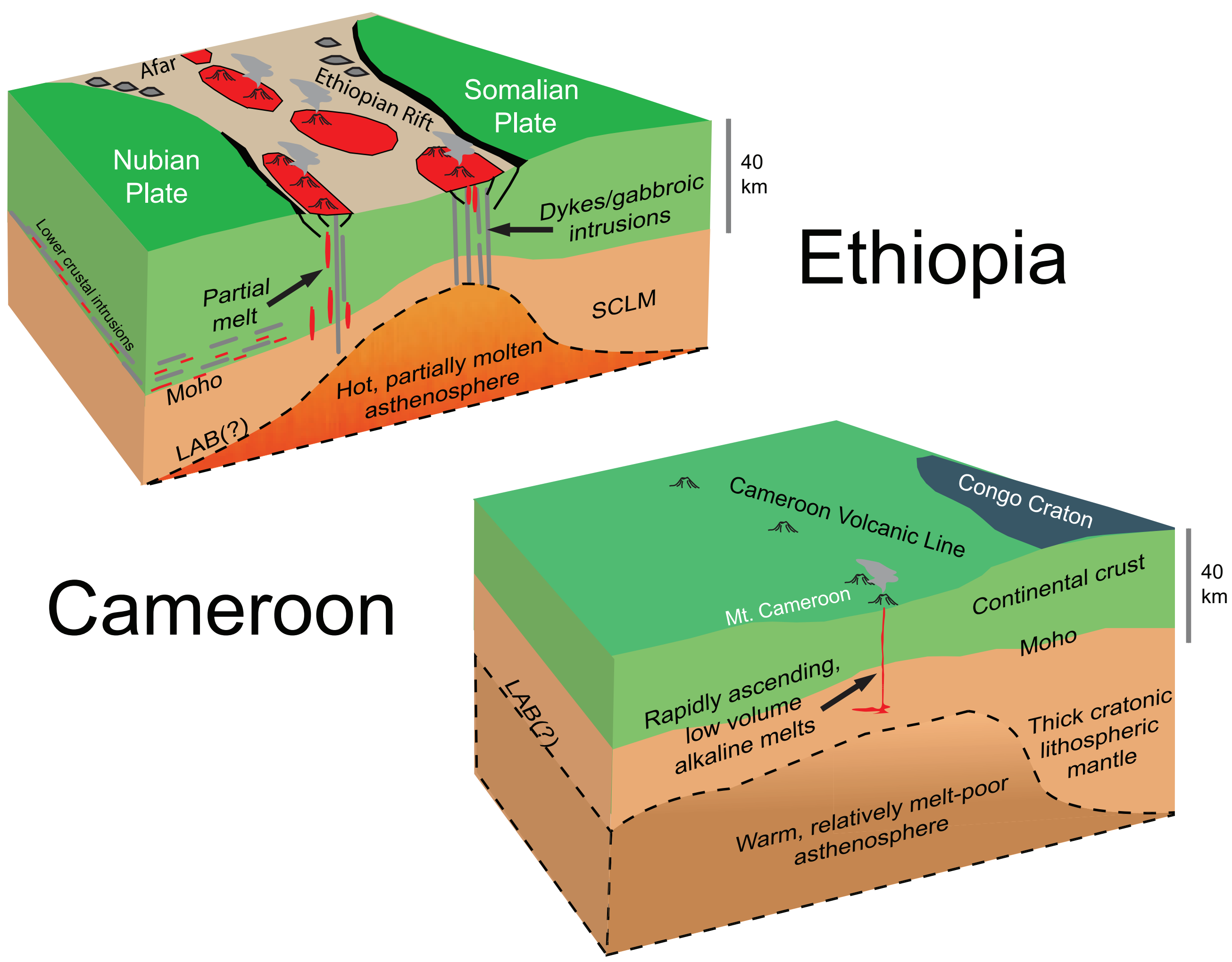
Afar
Ethiopian Rift
Somalian Plate
Nubian Plate
40 km
Dykes/gabbroic intrusions
Ethiopia
Lower crustal intrusions
Partial melt
SCLM
Moho
Hot, partially molten asthenosphere
LAB(?)
Cameroon Volcanic Line
Congo Craton
Cameroon
40 km
Mt. Cameroon
Continental crust
Moho
Rapidly ascending, low volume alkaline melts
LAB(?)
Thick cratonic lithospheric mantle
Warm, relatively melt-poor asthenosphere